TALLINNA TEHNIKAÜLIKOOL
INSENERITEADUSKOND
Ehituse ja arhitektuuri instituut

COMPARTMENT TEST WITH WOODEN I-JOISTS – ANALYSIS AND COMPARISON TO STANDARD FIRE

PUIDUST I-TALADEGA RUUMTULEKAHJUKATSE ANALÜÜS JA KAHJUSTUSTE VÕRDLUS STANDARDTULEKAHJUGA

MAGISTRITÖÖ

Üliõpilane: Mattias Mihkelson

Üliõpilaskood: 165193EAEI

Juhendaja: Katrin Nele Mäger, doktorant-nooremteadur

Kaasjuhendaja: Professor Alar Just

Tallinn 2023

(Tiitellehe pöördel)

AUTORIDEKLARATSIOON

Olen koostanud lõputöö iseseisvalt.
Lõputöö alusel ei ole varem kutse- või teaduskraadi või inseneridiplomit taotletud.
Kõik töö koostamisel kasutatud teiste autorite tööd, olulised seisukohad, kirjandusallikatest ja mujalt pärinevad andmed on viidatud.

"....." 2023

Autor: .....
/ allkiri /

Töö vastab bakalaureusetöö/magistritööle esitatud nõuetele

"....." 2023

Juhendaja: .....
/ allkiri /

Kaitsmisele lubatud

"....."..... 2023 .

Kaitsmiskomisjoni esimees .....
/ nimi ja allkiri /

Lihtlitsents lõputöö reprodutseerimiseks ja lõputöö üldsusele kättesaadavaks tegemiseks[1]

Mina, Mattias Mihkelson,

1. Annan Tallinna Tehnikaülikoolile tasuta loa (lihtlitsentsi) enda loodud teose "Puidust I-taladega ruumtulekahjukatse analüüs ja kahjustuste võrdlus standardtulekahjuga", mille juhendaja on Katrin Nele Mäger,

1.1 reprodutseerimiseks lõputöö säilitamise ja elektroonse avaldamise eesmärgil, sh Tallinna Tehnikaülikooli raamatukogu digikogusse lisamise eesmärgil kuni autoriõiguse kehtivuse tähtaja lõppemiseni;

1.2 üldsusele kättesaadavaks tegemiseks Tallinna Tehnikaülikooli veebikeskkonna kaudu, sealhulgas Tallinna Tehnikaülikooli raamatukogu digikogu kaudu kuni autoriõiguse kehtivuse tähtaja lõppemiseni.

2. Olen teadlik, et käesoleva lihtlitsentsi punktis 1 nimetatud õigused jäävad alles ka autorile.

3. Kinnitan, et lihtlitsentsi andmisega ei rikuta teiste isikute intellektuaalomandi ega isikuandmete kaitse seadusest ning muudest õigusaktidest tulenevaid õigusi.

_____ (kuupäev)

[1] *Lihtlitsents ei kehti juurdepääsupiirangu kehtivuse ajal vastavalt üliõpilase taotlusele lõputööle juurdepääsupiirangu kehtestamiseks, mis on allkirjastatud teaduskonna dekaani poolt, välja arvatud ülikooli õigus lõputööd reprodutseerida üksnes säilitamise eesmärgil. Kui lõputöö on loonud kaks või enam isikut oma ühise loomingulise tegevusega ning lõputöö kaas- või ühisautor(id) ei ole andnud lõputööd kaitsvale üliõpilasele kindlaksmääratud tähtajaks nõusolekut lõputöö reprodutseerimiseks ja avalikustamiseks vastavalt lihtlitsentsi punktidele 1.1. ja 1.2, siis lihtlitsents nimetatud tähtaja jooksul ei kehti.*

Ehituse ja arhitektuuri instituut

LÕPUTÖÖ ÜLESANNE

Üliõpilane: Mattias Mihkelson, 165193EAEI (nimi, üliõpilaskood)
Õppekava, peaeriala: EAEI02/15 – Ehitiste projekteerimine ja ehitusjuhtimine
Juhendajad: Katrin Nele Mäger, doktorant-nooremteadur
Professor Alar Just

Lõputöö teema:

Puidust I-taladega ruumtulekahjukatse analüüs ja kahjustuste võrdlus standardtulekahjuga

Compartment test with wooden I-joists – analysis and comparison to standard fire

Lõputöö põhieesmärgid:

1. Ruumtulekahju katsekeha ettevalmistus ja dokumenteerimine
2. Katseandmete analüüs
3. I-taladega ja massivpuidust sarnaste ruumtulekahjukatsete võrdlus
4. Puidust I-talade söestumissügavuste võrdlus tegelikus tulekahjus standardtulekahju arvutusmeetodiga
5. Järeldused ja ettepanekud Eurokoodeks 5-1-2 töörühmale (CEN TC250 SC5 WG4).

Lõputöö etapid ja ajakava:

Nr	Ülesande kirjeldus	Tähtaeg
1.	Katsekeha ettevalmistus	
2.	Kirjanduse ülevaade ja kokkuvõte analoogsetest katsetest massiivpuiduga	
3.	Katseandmete analüüs	
4.	Ruumtulekahju kahjustuste võrdlus standardtulekahjuga	
5.	Töö vormistamine	

Töö keel: Inglise **Lõputöö esitamise tähtaeg:** "06" jaanuar2023.a

Üliõpilane: Mattias Mihkelson ..... "....."..... 20…..a
/allkiri/

Juhendaja: Katrin Nele Mäger ..... "....."..... 20…..a
/allkiri/

Alar Just ..... "....."..... 20…..a
/allkiri/

CONTENTS

PREFACE

This thesis topic was suggested by my co-supervisor Alar Just. The compartment was built and tested in Tiller, Norway at RISE Fire Research AS after which the analysis and comparisons were made in Tallinn, Estonia.

I would like to express my gratitude towards everyone who has supported me throughout my studies. Special gratitude goes to my supervisor Katrin Nele Mäger for the continuous support and guidance. Also, I would like to show my appreciation towards Alar Just for introducing me to the world of timber structures.

In this thesis, a compartment fire with structural I-joists is built and analysed. Calculations of the I-joist charring depths are made according to prEN 1995-1-2:2025. The calculations and previous compartments tests of similar nature are compared to the conducted test.

Keywords: I-joist, fire design, compartment fire, charring, master's theses

LIST OF ABBREVIATIONS AND SYMBOLS

Latin upper-case letters

A	the area of cross-section
A_f	surface area of the compartment floor
A_t	total surface area of the enclosure incl. openings
A_v	total aera of vertical openings on all walls
GtA	gypsum plasterboard, Type A
GtC	gypsum plasterboard, Type C
GtF	gypsum plasterboard, type F
GtX	gypsum plasterboard, type X
T	temperature
T_0	initial temperature
O	opening factor of the fire compartment

Latin lower-case letters

b	width of the initial cross-section
b_{ef}	effective width of the effective cross-section
b_f	initial cross-section width of the flange
$d_{char,n}$	notional charring depth
$d_{char,n,1}$	notional charring depth for the fire exposed side
$d_{char,n,2}$	notional charring depth for the lateral side
h	height of the initial cross-section
h_f	initial cross-section height of the flange
h_i	thickness of layer *i*
h_p	thickness of the protective panel
h_{eq}	weighted average of window height on all walls
k_2	protection factor for Phase 2
$k_{3,1}$	post-protection factor for the fire exposed side
$k_{3,2}$	post-protection factor for the lateral side
k_4	consolidation factor for Phase 4
k_{gd}	modification factor considering grain direction
k_n	conversion factor
$k_{pos,exp,i}$	position coefficient that takes into account the influence of layers preceding the layer considered
$k_{pos,unexp,i}$	position coefficient that takes into account the influence of layers backing the layer considered

$k_{s,n,1}$	combined conversion and section factor for the fire exposed side
$k_{s,n,2}$	combined conversion and section factor for the lateral side
$q_{f,d}$	design fire load density related to the floor area A_f
$q_{t,d}$	design value of the fire load density related to the total surface area
t	time of fire exposure
t_a	time to reach the consolidated charring phase
t_{ch}	start time of charring
$t_{ch,2}$	start time of charring for the lateral side
$t_{f,pr}$	failure time of the fire protection system
t_{lim}	time for maximum gas temperature in case of fuel controlled fire
t_{max}	time for maximum gas temperature
$t_{prot,0,i}$	basic protection time of the considered layer *i*
$t_{prot,i}$	protection time of the considered layer *i*

Greek upper-case letters

Δt_i	correction time of the layer *i*
Θ_g	gas temperature in the fire compartment
$\Sigma t_{prot,i}$	sum of protection times

Greek lower-case letters

β_0	basic design charring rate
β_n	notional charring rate within one charring phase
λ	thermal conductivity of boundary of enclosure
ρ	density of boundary of enclosure

1. INTRODUCTION

Wood has been widely used as a construction material throughout history due to its availability. It is renewable, can be cut to the right size and can be used as is. One of the main advantages of wood is its strength relative to its weight compared to concrete or steel. Wood can be mixed with different additives like adhesives to make engineered wood. There are multiple ways that engineered lumber can be used.

Engineered lumber has been processed to perform in a different, better way than what sawn wood would perform. Engineered lumber can withstand a higher load when it is manufactured to do so. Different kinds of panels, and combinations of them are used as boards. By combining multiple layers of panels cross-laminated timber and glue-laminated timber can be produced. Using strands or wood particles from wood milling excess enables more raw material usage. When using wood with adhesives composite materials like wooden I-joists can be produced.

Due to wood being a combustible material, the research on engineered wood in natural fire situations is needed to create a reliable calculation model. The structural wood can be protected with different types of materials like gypsum and mineral wool.

There have been previous tests with the aim of researching the behaviour of wood in different fire situations. Due to the increasing popularity of engineered wood and building increasingly higher buildings with structural wooden components, the testing to create a reliable calculation model is needed.

The main aim of this thesis is to analyse a compartment fire test which was built with structural I-joists and to give feedback to the European design standard for timber structures draft prEN 1995-1-2:2025.

The main body of this thesis is divided into three larger parts. The first part is an overview of the calculation based on prEN 1995-1-1:2025 and a literature overview of previous compartment fire tests of similar nature. The second part is the design and description of the compartment which gives an overview of the compartment construction. The third part is the analysis of the data received from the compartment test. Calculations based on the standard draft and the input data from the fire test are performed. Comparisons are made between the test, previous research, and input from the design standard.

2. BACKGROUND

Wooden I-joists are wood-based composite materials. They are usually made of strength graded structural timber for the flanges and particle board or oriented strand board for the web. The I-joist height and width differ between factories. Wooden I-joists are intended for use as structural parts of a building construction. For example, they can be used as floor or roof beams, also as rafters. More recently, I-joists are increasingly used as wall studs.

There are multiple advantages of wooden I-joists compared to sawn wood. Compared to regular structural timber wooden I-joists are much easier to handle and install due to their low weight. Longer wood can be used due to less shrinkage and warp due to glued components. More elements of the log can be used in the construction because even the by-product of the sawmill is used. Limited holes can be cut in the web for utilities of the joist without endangering the structure. Thermally isolated constructions have fewer thermal bridges when using I-joists compared to traditional cut lumber. The main disadvantage of wooden I-joists is the possible failure in a fire when left unprotected compared to conventional timber.

There are different fires which are described with a temperature-time curve. A standard fire is the time-dependent temperature curve in which the temperature never drops. A parametric fire considers the geometry of the compartment, the openings, and the characteristics of the boundary of the enclosure, also the growth rate and the decay of the fire. A parametric time-temperature curve is much more comparable to a natural fire.

2.1 Fire design of timber structures

The fire design of timber structures is described in EN 1995-1-2 Eurocode 5 – design of timber structures Part 1-2: Structural fire design. This thesis uses the draft version prEN 1995-1-2:2025.
The charring depth is obtained using 300 °C isotherms. The char-line at different time values is assumed to be at that position. The Eurocode 5 includes the European charring model. The charring model should be applied to the standard fire exposure. [1]

2.1.1 The European charring model

The European charring model consists of multiple charring phases and should be taken into account where relevant [1]:

- **normal charring phase (Phase 1)** for initially unprotected sides of timber members and for initially protected sides of timber members,
- **encapsulated phase (Phase 0)** is the phase when no charring occurs behind the fire protection system,
- **protected charring phase (Phase 2)** is the phase when charring occurs behind the fire protection system while this system is still in place.
- **post-protected charring phase (Phase 3)** is the phase after the failure of the fire protection system before a fully developed char layer has been formed,
- **consolidated charring phase (Phase 4)** is the phase with fully developed char layer.

The phases are defined by a time period which express the characteristic events in each phase.

The charring depth of a timber member can be calculated with formula (2.1):

$$d_{char,n} = \beta_n t \tag{2.1}$$

where $d_{char,n}$ – the notional charring depth, mm,

β_n – the notional design charring rate, which includes the effect of corner roundings and fissures, mm/min,

t – the time of fire exposure, min. [1]

The notional design charring rate is calculated according to the formula (2.2) [1].

$$\beta_n = \prod \beta_0 k_i \tag{2.2}$$

where β_0 – the basic design charring rate, mm/min,

Πk_i – the product of applicable modification factors for charring.

For the calculation of the notional design charring rate of glulam using formula (2.2) the conversion factor and the grain direction factor were applicable for this thesis. The conversion factor k_n considers the effect of rounding of the linear member. The conversion factor for glulam linear members is k_n = 1,08. The grain direction factor considers the effect for charring perpendicular or parallel to the grain. In this thesis

only charring perpendicular to the grain happens and the value of the grain direction factor is k_{gd} = 1. [1]

The basic design charring rate β_0 value us obtained from prEN 1995-1-2:2025 in Table 5.3. The value for timber members made of softwood (incl. glulam and I-joist flange) is β_0 = 0,65 mm/min. [1]

For initially unprotected members the notional design charring rate can be calculated with the formula (2.3).

$$\beta_n = k_{gd} k_n \beta_0 \tag{2.3}$$

2.1.2 Fire design of I-joists

The fire design calculation of I-joists are provided in Annex I of prEN 1995-1-2:2025 which is based on the research of Alar Just and Katrin Nele Mäger [2] [3]. The annex and previous research provide the design rules for timber frame assemblies with linear I-shaped members.

Based on the prEN1995-1-2:2025 charring of the timber member should be taken from the fire exposed side and when relevant from the lateral side depending on the protective ability of the fire protection system and the protection level of the cavity insulation as seen in Figure 2.1 and Figure 2.2. The cavity insulation based on the European standard used in this thesis is of a Protection level 1 (PL1) which means that stone wool with a density higher than 26 kg/m^3 is used in the cavities and that the charring develops primarily on the fire exposed side of the timber, while lateral sides are semi-protected from the heat. [1]

The Annex I presents three design models for I-shaped members of timber frame assemblies [1]:

- charring phases with cavity insulations qualified as PL1 and PL2 when charring on the lateral side occurs before the failure of fire protection system; $t_{ch,2} \leq t_{f,pr}$; as seen in Figure 2.1;
- charring phases with cavity insulations qualified as PL1 and PL2 when charring on the lateral side occurs after the failure of fire protection system; $t_{ch,2} > t_{f,pr}$; as seen in Figure 2.2;
- charring phases for void cavities; not applicable in this thesis.

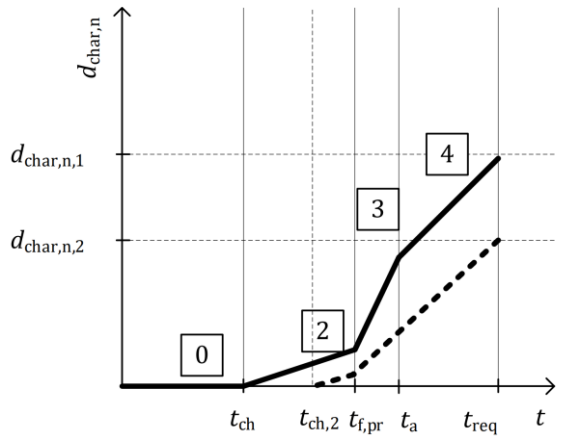

Figure 2.1 Design model for I-shaped timber members of timber frame assemblies when charring on the lateral side occurs before the failure of fire protection system [1]

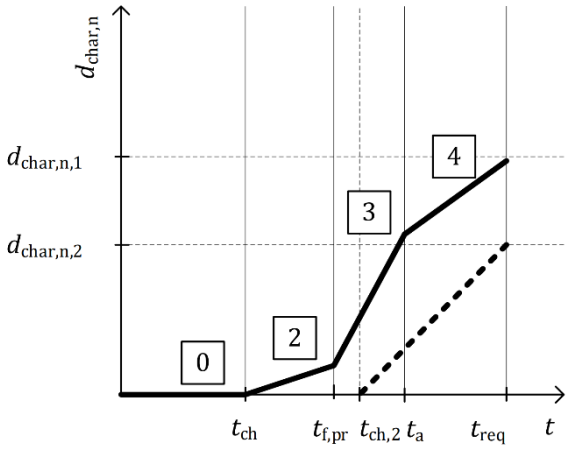

Figure 2.2 Design model for I-shaped timber members of timber frame assemblies when charring on the lateral side occurs after the failure of fire protection system [1]

In the Figure 2.1 and Figure 2.2 numbers in the rectangular box correspond to the charring phase. Other values are as follows:

t_{ch} – start time of charring on the fire exposed side, min,

$t_{ch,2}$ – start time of charring on the lateral side, min,

$t_{f,pr}$ – failure time of the fire protection system, min,

t_a – consolidation time, min,

t_{req} – required time of fire resistance, min,

$d_{char,n,1}$ – notional charring depth at fire exposed side, mm,

$d_{char,n,2}$ – notional charring depth at lateral side, mm. [1]

The effective cross-section depth of the flange can be calculated according to the formula (2.4) [1].

$$h_{f,ef} = h_f - d_{ef} \tag{2.4}$$

where $h_{f,ef}$ – the effective cross-section depth of the flange, mm,

h_f – the initial cross-section depth of the flange, mm,

d_{ef} – effective charring depth, mm.

The effective charring depth can be calculated by the formula (2.5).

$$d_{ef} = d_{char,n,1} + d_0 \tag{2.5}$$

where $d_{char,n,1}$ – the notional charring depth of the fire exposed side of the flange, mm,

d_0 – the zero-strength layer depth.

In this thesis the zero-strength layer depth is not calculated. Only the charring depth of the cross-sections are determined for comparable results to the compartment test.

The notional charring depth $d_{char,n,1}$ for the fire exposed side and $d_{char,n,2}$ for the lateral side should be calculated as follows [1]:

$$d_{char,n,1} = \sum_{Phases} (\beta_n \cdot t) \tag{2.6}$$

$$d_{char,n,2} = \sum_{Phases} (\beta_n \cdot t) \tag{2.7}$$

where β_n – is the notional charring rate within one charring phase according to equations (2.8) to (2.12), mm/min.

The notional charring rates of the I-shaped timber members should be calculated as follows [1]:

Phase 2	$\beta_n = k_2 \cdot k_{s,n,1} \cdot \beta_0$	for the fire exposed side	(2.8)
Phase 2	$\beta_n = k_2 \cdot k_{s,n,2} \cdot \beta_0$	for the lateral side	(2.9)
Phase 3	$\beta_n = k_{3,1} \cdot k_{s,n,1} \cdot \beta_0$	for the fire exposed side	(2.10)
Phase 3	$\beta_n = k_{3,2} \cdot k_{s,n,2} \cdot \beta_0$	for the lateral side	(2.11)
Phase 4	$\beta_n = k_4 \cdot k_{s,n,1} \cdot \beta_0$	for the fire exposed side	(2.12)

where $k_{s,n,1}$ – the combined conversion and section factor for the fire exposed side according to (2.13),

$k_{s,n,2}$ – the combined conversion and section factor for the lateral side according to (2.14),

k_2 – the protection factor for Phase 2 according to (2.15),

$k_{3,1}$ – the post-protection factor for Phase 3 for the fire exposed side according to (2.16),

$k_{3,2}$ – the post-protection factor for Phase 3 for the lateral side according to (2.17),

k_4 – the factor for Phase 4 according to (2.18).

The combined conversion and section factor $k_{s,n,1}$ for the fire exposed side and $k_{s,n,2}$ for the lateral side with PL1 insulation are calculated according to the following equations [1]:

$$k_{s,n,1} = 9{,}48 \cdot b_f^{-0{,}43} \tag{2.13}$$

$$k_{s,n,2} = 2{,}25 \cdot h_f^{-0{,}13} \tag{2.14}$$

where b_f – the initial cross-section width of the flange, mm,

h_f – the initial cross-section depth of the flange, mm.

In this thesis gypsum plasterboard is used to protect the wooden I-joists. Based on that, the protection factor k_2 is calculated according to the following formula:

$$k_2 = 1 - \frac{h_p}{55} \tag{2.15}$$

where h_p – the thickness of the single panel or the total thickness of multiple panels of the same material, mm. [1]

In this thesis the post-protection factor for Phase 3 is only calculated for the flange with cavities filled with PL1 mineral wool. The post-protection factor $k_{3,1}$ for the fire exposed side and $k_{3,2}$ for the lateral side are calculated according to formulae (2.16) and (2.17). [1]

$$k_{3,1} = 6{,}5 - \frac{t_{f,pr}}{25} \tag{2.16}$$

$$k_{3,2} = 0{,}01 + \frac{\max\left(t_{f,pr}; t_{ch,2}\right)}{338} \tag{2.17}$$

For Phase 4, the factor k_4 for the fire exposed side is calculated according to formula (2.18). [1]

$$k_4 = 0{,}9 + \frac{t_a}{48} \tag{2.18}$$

For the cavity insulation PL1 The consolidation time t_a is calculated according to the formula (2.19). [1]

$$t_a = 1{,}04 \cdot t_{f,pr} \tag{2.19}$$

The start time of charring for the lateral side of the timber member flange $t_{ch,2}$ is calculated according to the formula (2.20). [1]

$$t_{ch,2} = \sum t_{prot,i-1} + t_{prot,i} \tag{2.20}$$

where $\sum t_{prot,i-1}$ – the sum of the protection times of the layers preceding the insulation layer *i*, min,

$t_{prot,i}$ – the protection time of the layer *i* with thickness h_f calculated according to (2.21), min.

2.1.3 Separating function method – protection time

The protection time of timber members are calculated as the time from the start of charring until the member is completely charred in the direction of the heat flux. The protection time $t_{prot,i}$ for panels and insulation products are calculated according to formula (2.21). [1]

$$t_{prot,i} = (t_{prot,0,i} \cdot k_{pos,exp,i} \cdot k_{pos,unexp,i} + \Delta t_i) \cdot k_{j,i} \tag{2.21}$$

where $t_{prot,0,i}$ – the basic protection time of considered layer *i*, min,

$k_{post,exp,i}$ – the position coefficient that takes into account the influence of layers preceding the layer considered,

$k_{post,unexp,i}$ – the position coefficient that takes into account the influence of layers backing the layer considered,

Δt_i – the correction time for considered layer *i*, min,

$k_{j,i}$ – the joint coefficient for layer *i*.

The basic protection time for gypsum plasterboard is calculated with formula (2.22) and mineral wool insulation PL1 with a thickness more than 40 mm is calculated according to (2.23). [1]

$$t_{prot,0,i} = 30\left(\frac{h_i}{15}\right)^{1,2} \tag{2.22}$$

where h_i – the thickness of the considered layer, mm.

$$t_{prot,0,i} = 0{,}3 \cdot h_i^{\left(0{,}75 \cdot log(\rho_i) - \frac{\rho_i}{400}\right)} \tag{2.23}$$

where ρ_i – density of the considered layer, kg/m^3.

For 2 layers of gypsum plasterboard of type F, the basic protection time $t_{prot,0,i}$ in formula (2.22) is calculated with the thickness h_i according to the formula (2.24). [1]

$$h_i = h_1 + 0{,}8 \cdot h_2 \tag{2.24}$$

where h_1 is the thickness of the gypsum board on the fire exposed side.

The position coefficient for the fire exposed side $k_{pos,exp,i}$ is calculated according to the formula (2.25). [1]

$$k_{pos,exp,i} = 0{,}5\sqrt{\frac{t_{prot,0,i}}{\sum t_{prot,i-1}}} \tag{2.25}$$

The formula (2.25) is only to be used in cases where the product of the layer is one of the following: panel or panelling made of timber or gypsum; clay and lime plaster, clay boards; mineral wool insulation PL1. The second condition is that the sum of protection times of preceding layers must be bigger than the half of the basic protection time of the considered layer. If the considered layer is the first layer, then $k_{pos,exp,i} = 1$. [1]

The position coefficient $k_{pos,unexp,i}$ for the unexposed side for layers backed by insulation is calculated with formula (2.26) or (2.27), depending on the product. [1]

Gypsum plasterboard $$k_{pos,unexp,i} = 0{,}5 \cdot h_i^{0,15} \tag{2.26}$$

Mineral wool PL1 $$k_{pos,unexp,i} = 0{,}18 \cdot h_i^{(0{,}001\rho_i + 0{,}08)} \quad (2.27)$$

The influence of a void cavity with a thickness less than 40 mm is neglected. [1]

The correction time Δt_i is added to all layers behind the panels, if the sum of protection times of the preceding layers and the panels is less than the failure time of the panel or the fire protection system including the panels [1]. The increased effect of protection provided by panels should be taken into account by adding the correction time to the protection or insulation time of layers behind the panels [1]. If the layer *i* is the first layer, then $\Delta t_i = 0$ min because there are no preceding layers.

The correction time Δt_i of the layer *i* should be calculated as follows [1] (as seen in Figure 2.1):

$$\Delta t_i = \frac{\left(t_{f,pr} - \sum t_{prot,i-1}\right)}{t_{prot,max,i}} \leq \Delta t_{max,i} \quad (2.28)$$

where $\Delta t_{max,i}$ – the maximum correction time of the layer *i*, min,

$t_{prot,max,i}$ – the maximum protection time of the layer *i*, min.

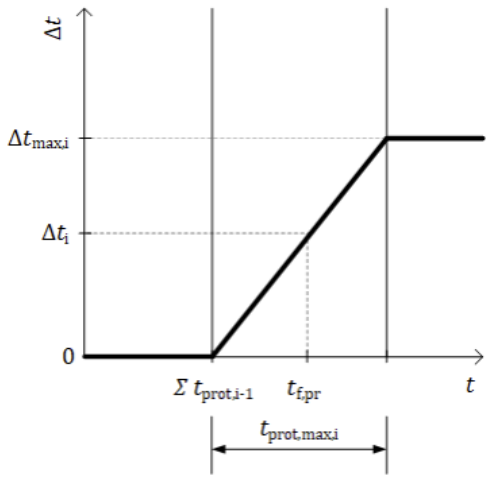

Figure 2.3 Limits of the correction time [1]

The maximum protection time $t_{prot,max,i}$ of the layer *i* is calculated according to the formula (2.29). [1]

$$t_{prot,max,i} = \frac{t_{prot,0,i}}{k_2} \quad (2.29)$$

where k_2 – the protection coefficient for the panel or the fire protection system preceding the layer *i*.

The maximum correction time $\Delta t_{max,i}$ of the layer *i* is calculated according to the formula (2.30). [1]

$$\Delta t_{max,i} = t_{prot,max,i} - t_{prot,0,i} \cdot k_{pos,exp,i} \cdot k_{pos,unexp,i} \cdot k_{j,i} \quad (2.30)$$

The joint coefficient $k_{j,i}$ for the layer backed by batten, panel, timber member, insulation or void cavity with a thickness less than 40 mm should be assumed with a value $k_{j,i} = 1$. [1]

2.2 Fire scenarios

Due to the need of a standardised fire exposure, there are multiple time-temperature curves that can be used. The prEN 1995-1-2 refers to the standard fire exposure as seen in Figure 2.4. The standard fire according to ISO 834 [4] is a special case of natural fire. The standard fire is described with formula (2.31) [5]. This time-temperature curve allows to compare multiple fire tests. The standard time-temperature curve is depicted in Figure 2.4. The curve does not account for fire load, openings, thermal or insulating properties of the compartment. Also, there is no decay or extinguishing phase – the fire temperature keeps rising for an unlimited duration.

$$T = T_0 + 345 log_{10}(8t + 1) \quad (2.31)$$

where T – temperature at time t, °C,
T_0 – initial temperature, °C,
t – time, min.

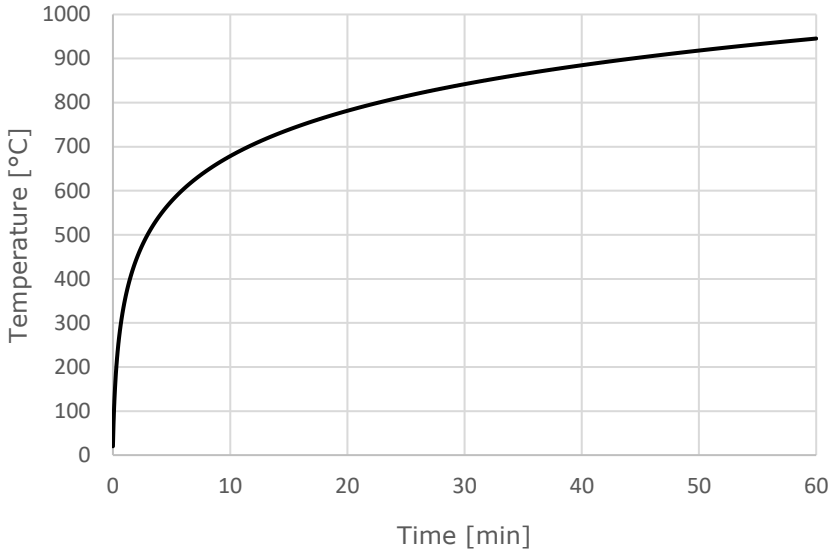

Figure 2.4 ISO 834 Standard temperature-time curve [4]

The standard temperature-time curve from ISO 834 does not describe a real-life natural fire and cannot be compared directly to a natural fire. A more comparable temperature-time curve for compartments can be found in EN 1991-1-2:2002.

Parametric fire curves for compartments can be based on Annex A in EN 1991-1-2:2004 Eurocode 1: Part 1-2. The described temperature-time curve is valid for fire compartments up to 500 m^2 of floor area, without openings in the roof and for a maximum compartment height of 4 m [5].This temperature-time curve is described in two phases: a heating phase and a cooling phase. For the heating phase the gas temperature in the compartment can be calculated according to the following formula [5]:

$$\Theta_g = 20 + 1325\,(1 - 0{,}324e^{-0{,}2t^*} - 0{,}204e^{-1{,}7t^*} - 0{,}472e^{-19t^*}) \qquad (2.32)$$

where Θ_g – the gas temperature in the fire compartment, °C,

$t^* = t \cdot \Gamma$, h,

$\Gamma = [O/b]^2 / (0{,}04/1160)^2$, -,

$b = \sqrt{(\rho c \lambda)}$, J/($m^2 s^{1/2} K$),

ρ – density of boundary of enclosure, J/kgK,

c – specific heat of boundary of enclosure, W/mK,

λ – thermal conductivity of boundary of enclosure, W/mK,

O – opening factor, $m^{1/2}$.

The opening factor O represents the amount of ventilation depending on the area of openings in the compartment walls, the height of these openings and the total area of enclosure surfaces. The bigger the opening factor value is the more the fire is ventilation controlled. The opening factor is calculated according to formula (2.33) [5].

$$O = A_v\sqrt{h_{eq}}/A_t \tag{2.33}$$

where O – opening factor of the fire compartment, $m^{1/2}$,

A_v – total area of vertical openings on all walls, m^2,

h_{eq} – weighted average of window heights on all walls, m,

A_t – total area of enclosure (walls, ceiling and floor, including openings), m^2.

The maximum temperature in the heating phase happens at the time t_{max} which is calculated according to (2.34).

$$t_{max} = \max\left(\left(0{,}2 \cdot 10^{-3}\frac{q_{t,d}}{O}\right); t_{lim}\right) \tag{2.34}$$

where q_{td} – the design value of the fire load density related to the total surface area A_t and calculated according to (2.35)(2.37), MJ/m^2.

$$q_{td} = q_{f,d} \cdot \frac{A_f}{A_t} \tag{2.35}$$

where $q_{f,d}$ – the design value of the fire load density related to the surface area of the floor, MJ/m^2,

A_f – floor area of the compartment, m^2.

In case the fire is fuel controlled then t_{max} is given by t_{lim}. If the growth of the fire is slow, t_{lim} = 25 min, if the fire is of medium growth, t_{lim} = 20 min and in case of a fast fire growth rate, t_{lim} = 15 min. [5]

The temperature-time curve in the cooling phase is calculated with one of the following equations which depend on the modified time of fire duration t^*_{max}. [5]

$$t^*_{max} \leq 0{,}5 \qquad \Theta_g = \Theta_{max} - 625(t^* - t^*_{max} \cdot x) \tag{2.36}$$

$$0{,}5 < t^*_{max} < 2 \qquad \Theta_g = \Theta_{max} - 250(3 - t^*_{max})(t^* - t^*_{max} \cdot x) \tag{2.37}$$

$$t^*_{max} \geq 2 \qquad \Theta_g = \Theta_{max} - 250(t^* - t^*_{max} \cdot x) \tag{2.38}$$

3. LITERATURE OVERVIEW OF COMPARTMENT FIRE TESTS

Multiple compartment fire tests with wood have been conducted throughout the last 20 years. Every performed test and the examination of results provides more information on the behaviour of wood in a more realistic fire environment. This paragraph presents a short overview of compartment fire tests which are comparable to the one conducted for this thesis. An overview of the comparable tests is given in Table 3.1. The results of the tests are covered in Table 3.2. These tables are reproduced from the report "Fire Safety Challenges of Tall Wood Buildings – Phase 2: Task 1 – Literature Review" by Daniel Brandon and Birgit Östman [6].

Hakkarainen conducted four different compartment tests of which one used light timber framing and the others used heavy laminated timber. The compartment sizes were all 3,5 x 4,5 x 2,5 m with an opening of 2,3 x 1,2 m. The fire load density of the compartments were 900 MJ/m^2 without assuming the combustion efficiency of 0,8. [7]

The first test had fully exposed ceilings and walls. For the second test a single layer of 12,5 mm type A gypsum was used to protect the timber elements. The final two had a protection system consist of a layer of 12,5 mm gypsum type A (GtA based on [8]) and 15,4 mm gypsum type F (GtF). [7]

Two first tests showed relatively low compartment temperatures – about 700 °C due to under ventilation of the fire. Neither of the fires were showing decay so after 50 minutes the fire was stopped due to excessive flaming and a faulty smoke venting system. The third and fourth test had a higher peak temperature at about 1100 °C. The gypsum plasterboards remained intact during the high temperature period. A decay of fire was noted due to dropping temperature. The fourth test was stopped after 48 minutes because the ceiling was burning through. [7]

Lennon conducted three large scale natural fire tests on engineered timber. The aim of his research was to investigate the performance of new timber floor system products in a natural fire scenario. He observed three types of floor systems: solid timber floor joists, wooden I-joists and timber trusses which incorporated solid timber flanges with a pressed steel web. [9]

The compartment walls were built from concrete blocks. The floor was constructed with engineered lumber which was exposed to the fire. The dimensions of the

compartment were 4,0 x 3,0 x 2,4 m with two openings with a size of 0,7 x 1,0 m. The first test used solid timber floor joists, second engineered I-joists and the third engineered truss joists. A distributed load of 0,75 kN/m^2 was applied on top of the floor to resemble a typical load of a residential building. The solid timber joists were protected by 12,5 mm type F gypsum boards and the engineered timber joists were protected by 15 mm type F gypsum boards. The floors were designed to have 60 minutes of fire resistance in accordance with the UK building regulations. The temperatures were measured with type K thermocouples in the compartment and in the floor at different depths of the joists. Wooden pallets which provided a fire load density of 450 MJ/m^2 were used in each test. [9]

The temperatures had a peak of approximately 1000 °C during the three tests. The test concluded that engineered timber floors may be able to have the same fire resistance provided that the joists are protected against fire. The thicker 15 mm gypsum boards were more efficient in protecting the engineered floor joists compared to the 12.5 mm gypsum boards which were protecting the solid timber joists. [9]

McGregor, Li et al and Medina Hevia constructed all the compartments with the same geometry. This was to compare similar compartments to each other. The floor area of the compartments was 3,5 x 4,5 m with a height of 2,5 m. The compartments had one opening of a size 2,0 x 1,1 m. [10]

McGregor had walls, floors and ceiling made of 105 mm thick 3-ply CLT with lamellas of 35 x 89 mm. The aim of McGregor's research was to observe the performance and behaviour of CLT panels when exposed to different fires. McGregor conducted five similar tests with different fuel types. Using gas allowed to specify the contribution of CLT to the heat release rate. In three of the tests McGregor used furniture as fuel. Two of the tests had fully protected CLT walls and in one of the tests all the CLT was left unprotected. [11]

Gas temperature in the compartment as well as temperatures inside the ceiling and walls in varying depths were measured. Gas analysis of all extracted gas was performed to determine the heat release rate of the fire. In half of the tests the CLT was protected by two layers of GtF. [11]

McGregor assumed that the fully protected CLT does not contribute to the compartment fire. The assumption was confirmed after comparing the propane fuelled tests to the protected furniture ones.

Li et al did three tests with light timber frames and light steel frames with the same size and comparable fire loads as McGregor. Results of the tests which McGregor did with furniture fire loads were used as comparison. One compartment had a light steel frame which was covered by a layer of 12,5 mm Type C gypsum board which is similar to GtF but with added glass fibers. A similar test was conducted using timber studs instead of steel studs. The third test was similar to the second test but with two layers of gypsum board were used to protect the timber frame. All cavities were fully insulated with fibreglass (glass wool). CLT was used outside of the light frames to insure the structural stability of the frames during the fires. [12]

Li found that the temperature curves and heat release rate (HRR) were similar in the tests which used protected CLT. The test with unprotected CLT had higher HRR and slightly lower temperatures. After review it was determined that the increase in HRR was due to external burning of the compartment. The other tests did not have this due to under-ventilated burning conditions. The tests with two layers of gypsum protected the structural parts of the compartments. It was noted that the gypsum had better protection effect on CLT walls than in light frame walls due to the tight connection between the CLT that avoided the heat penetration. [12]

The light timber frames which were used in the tests had charring behind the gypsum boards. Combustion was noted before the failure of the protection system. The average charring rate was 1,22 mm/min based on a 30 mm charring depth. Li concluded that the fire performance of building elements in a natural fire may be different from the information obtained from in a standard test. [12]

Medina Hevia performed three compartment fire tests. The aim of the work was to study the contribution of CLT to a compartment fire corresponding to different configurations of protected and unprotected CLT surfaces. Furniture was used as fuel and placed in the same position as in the test series by McGregor to ensure a comparable result. [10]

Hevia concluded that unprotected CLT contributes to the fire growth rate, the intensity and the duration. The contribution of the CLT is more significant when there is more unprotected surface exposed to the fire. [10]

The following tables categorizes the main structural members as light timber frames (LTF), light steel frames (LSF), cross-laminated timber (CLT), heavy laminated timber (HLT).

Table 3.1 Overview of natural fire compartment tests [6]

Test	Reference	Floor area (m^2)	Opening area (m^2)	Opening factor ($m^{1/2}$)	Gypsum used	Main Structural members	Fuel type	Fire load density (MJ/m^2)
Ha1	Hakkarainen [7]	15,75	2,76	0,042	None	HLT	Wood cribs	900
Ha2		15,75	2,76	0,042	12,5 mm GtA	HLT	Wood cribs	900
Ha3		15,75	2,76	0,042	12,5 mm GtA 15.4 mm GtF	HLT	Wood cribs	900
Ha4		15,75	2,76	0,042	12,5 mm GtA 15,4 mm GtF	LTF	Wood cribs	900
Le1	Lennon [9]	12,00	1,40	0,024	2x12,5 mm GtF	LTF	Wood cribs	450
Le2		12,00	1,40	0,024	2x15 mm GtF	LTF	Wood cribs	450
Le3		12,00	1,40	0,024	2x15 mm GtF	LTF	Wood cribs	450
Mc1	McGregor [11]	15,75	2,14	0,042	2x12,7 mm FR	CLT	Propane	486
Mc2		15,75	2,14	0,042	2x12,7 mm FR	CLT	Furniture	533
Mc3		15,75	2,14	0,042	None	CLT	Propane	182
Mc4		15,75	2,14	0,042	2x12,7 mm FR	CLT	Furniture	553
Mc5		15,75	2,14	0,042	None	CLT	Furniture	529
Li1	Li et al. [12]	15,75	2,14	0,042	2x12,5 mm GtC	LTF	Furniture	614
Li2		15,75	2,14	0,042	12,5 mm GtC	LTF	Furniture	610
Li3		15,75	2,14	0,042	12,5 mm GtC	LSF	Furniture	601
Me1	Medina Hevia [10]	15,75	2,14	0,042	63% of surface: 2x12,7 mm GtX	CLT	Furniture	532
Me2		15,75	2,14	0,042	58% of surface: 2x12,4 mm GtX	CLT	Furniture	532
Me3		15,75	2,14	0,042	79% of surface: 2x12,4 mm GtX	CLT	Furniture	532

Table 3.2 Overview of the test results [6]

Test	Opening factor ($m^{1/2}$)	Main Struc-tural mem-bers	Fire load density (MJ/m^2)	Test duration (min)	Time to flashover (mm:ss)	Approx. peak temp (°C)	Start of decay (min)	Gypsum used, mm (type)	Fall off time, (min)
Ha1	0,042	HLT	900	50	04:50	1100	No decay	None	N.A.
Ha2	0,042	HLT	900	46	04:30	1000	No decay	12,5 (GtA)	13
Ha3	0,042	HLT	900	169	06:00	1200	35	12,5 (GtA) 15,4 (GtF)	1: 27 2:>169
Ha4	0,042	LTF	900	48	06:10	1200	36	12,5 (GtA) 15,4 (GtF)	1: 32 2: N.F.
Le1	0,024	LTF	450	56	19:00	1084	40	2x12,5 (GtF)	2: 30
Le2	0,024	LTF	450	>60	20:00	1034	52	2x15 (GtF)	-
Le3	0,024	LTF	450	56	19:00	1036	No decay	2x15 (GtF)	2: 40
Mc1	0,042	CLT	486	119	04:57	1150	25	2x12,7 (FR)	2: 107
Mc2	0,042	CLT	533	53	07:30	N.A.	24	2x12,7 (FR)	1: 37,1 2: >53
Mc3	0,042	CLT	182	53	04:55	980	45	None	N.A.
Mc4	0,042	CLT	553	53	09:26	1000	26	2x12,7 (FR)	1: 39 2: >53
Mc5	0,042	CLT	529	63	05:00	1000	No decay	None	N.A.
Li1	0,042	LTF	614	42,5	06:12	1150	25	2x12,5 (GtC)	1: 35 2: 42,5
Li2	0,042	LTF	610	74	05:40	1150	25	12,5 (GtC)	44
Li3	0,042	LSF	601	47	08:00	1200	25	12,5 (GtC)	23,5
Me1	0,042	CLT	532	120	04:00	1200	20	63% of surface: 2x12,7 (GtX)	2: 72
Me2	0,042	CLT	532	56	05:00	1100	20	58% of surface: 2x12,4 (GtX)	1: 27 2: 45
Me3	0,042	CLT	532	81	06:00	1100	20	79% of surface: 2x12,4 (GtX)	1: 25 2: 45

4. TEST DESCRIPTION

As part of this thesis work one compartment fire test was conducted. The authors part in the compartment test was to assist building the compartment. The author drilled holes in the I-joists for thermocouples and helped connect them to the logger. The author assisted with the assembly of the framing and installing the mineral wool, gypsum boards and floor joists. The process of building the compartment took 4 full workdays.

4.1 Specimen

To conduct the test, a compartment was built in Tiller, Norway at the RISE Fire Research test centre in a large fire test hall. The walls and the ceiling were built from wooden I-joists produced by Masonite Beams AB. The compartment is meant to illustrate a room in a high-rise building.

The joists and sills were attached to each other by 5,0x100 screws. The sills were Masonite Beams S200 and the joists were H200. The ceiling beams had two particleboard squares added to the wall of the beam on both ends to fasten them to the edge beams. This is to reinforce the web of the I-joist [13]. The ceiling had wooden laths (22x70 mm) with a step of 400 mm which were nailed to the underside of I-beams with 2,8x75 nails. Then the laths were covered with one layer of GtA and on top of that a layer of GtF The layout of GtF was different from the GtA to ensure the joints were staggered. On the inside, the walls were covered with one layer of Type F gypsum board. All the GtA was fastened with 50 mm staples. The GtF was fastened with 63 mm staples. The floor was covered with hard stone wool boards, and it was then covered by GtF. The gypsum joints were plastered, corners were filled with fire sealant. All cavities between boards and I-joists were completely insulated with stone wool. The batts were mostly pre-cut into the right shape and put between the I-joists. In gaps smaller than the standard 600 mm step, the stone wool was cut into the right shape by hand to ensure a tight fit. The sections of the ceiling and wall can be seen in Figure 4.1.

On the outside the compartment walls were covered by 9 mm outdoor gypsum boards. The ceiling was covered with 10mm particleboard. The compartment had an opening 1.6 m wide and 2 m tall.

Two glulam timber (GLT) columns were installed in the back corners of the compartment. They were brought away from both walls by approximately 5 cm. The GLT was wedged between the ceiling and the floor with GtF spacers. In Figure 4.2 to Figure 4.5 the building of the compartment can be seen.

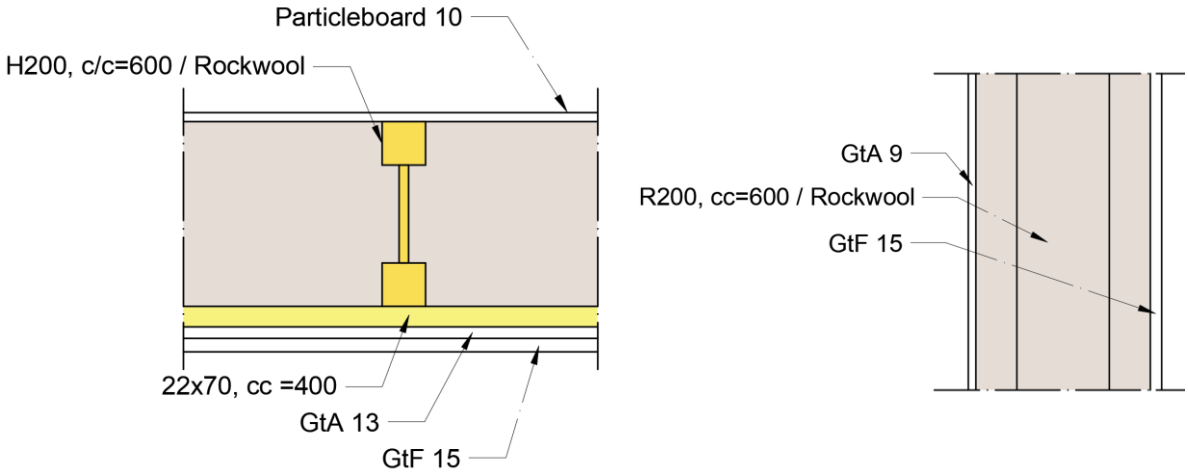

Figure 4.1 LEFT: Ceiling section; RIGHT: Wall section

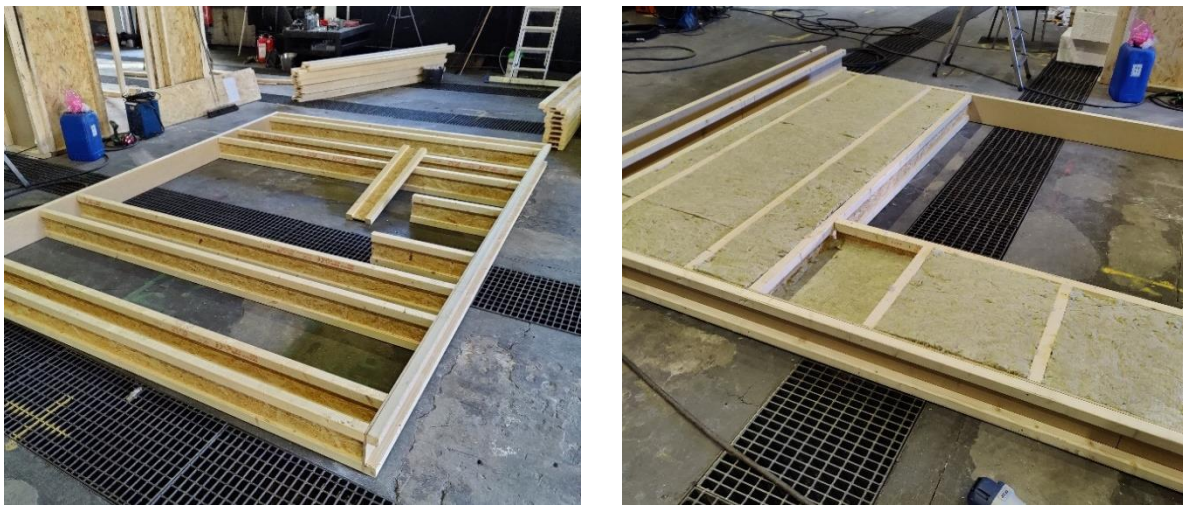

Figure 4.2 LEFT: Wall framing; RIGHT: Insulating the cavities

Figure 4.3 LEFT: Erected walls; RIGHT: Ceiling gypsum installation


Figure 4.4 LEFT: Ceiling without insulation; RIGHT: Insulating the cavities

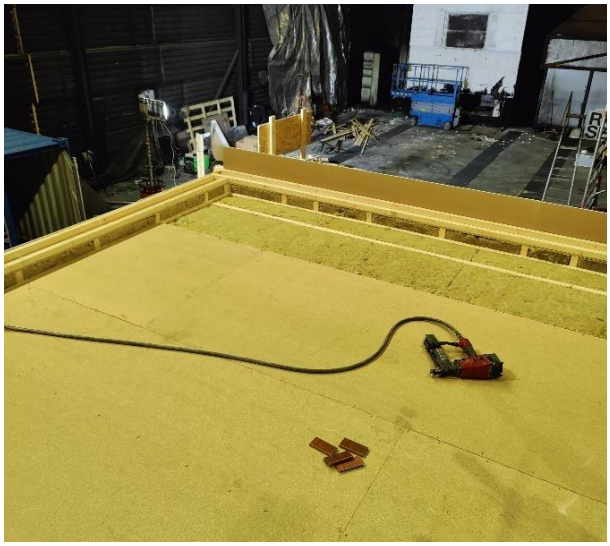


Figure 4.5 LEFT: Particleboard installation; RIGHT: Inside the finished compartment

4.2 Instrumentation

The measurement instruments used in the compartment test were provided by RISE Fire research AS. The following instrumentation was used in the compartment test:

- Data logger – measured data every 1.4 seconds
- Thermocouple – type K 1.5 mm according to IEC 584 [14]. About 5 mm of the isolation was removed from the tip. The end of the thermocouple had twisted tips.
- Plate thermometer – 7 meters away from opening, approx. 2 meters high, used for heat flux calculation.
- Heat sensor – measuring the heat flux of the compartment fire in the same position as the plate thermometer.
- TC tree - sheathed 1.5mm thermocouples type K according to IEC 584 [14].

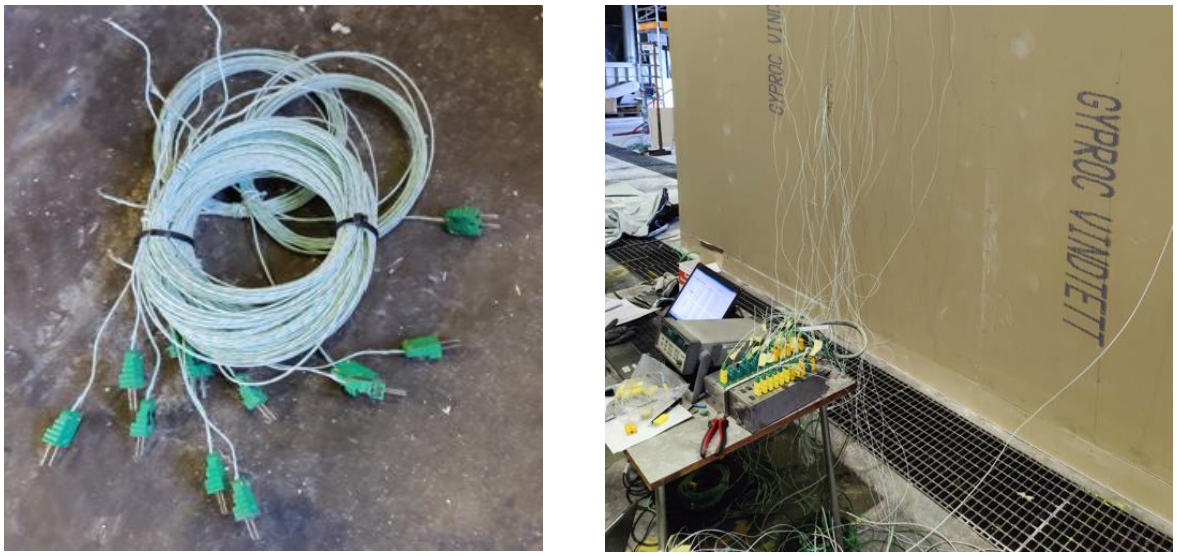

Figure 4.6 LEFT: Thermocouples with twisted tips; RIGHT: Instrumentation wiring

4.2.1 Thermocouple locations

During the construction of the compartment thermocouples were added in the wall and ceiling.

One I-joist in each wall except the opening wall and one ceiling beam had thermocouples drilled in at different distances from the fire exposed side of the flange as shown in Figure 4.7. Position X is to be changed with the according wall or roof position numbers.

The thermocouples in the flanges were drilled from the lateral side of the flange. The depths of the thermocouples from the fire exposed side were as following: x-2 at 6 mm depth, x-3 at 12 mm depth and x-4 at 18 mm depth. The joists with the thermocouples were at the plastered gypsum joints.

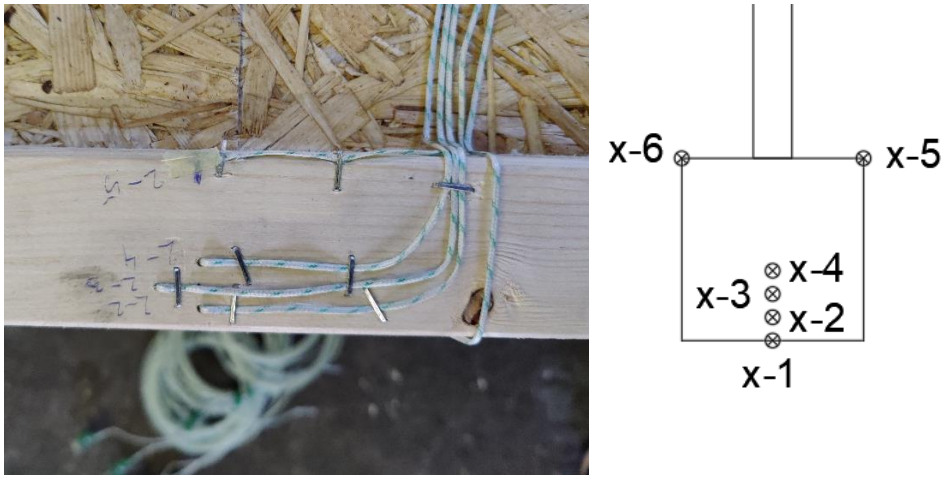

Figure 4.7 LEFT: Thermocouples in the I-joist; RIGHT: TC positions in the I-joist

The thermocouples in the cross sections were installed before the joists were fastened to the sills. The thermocouples in different layers of the wall were placed after the walls were lifted to place. A plan with the locations of the thermocouples in the walls can be seen in Figure 4.8. The walls are marked as following: left wall YV2, middle back wall YV3 and right wall YV4. All of the thermocouples in the walls were placed at a height of approximately 1.5 m from the ground.

There were in total twelve thermocouples (numbers 18 to 29) placed on top of the ceiling gypsum as seen in Figure 4.9. The thermocouples with numbers 6 to 11 are of the ceiling I-joist as seen in Figure 4.7.

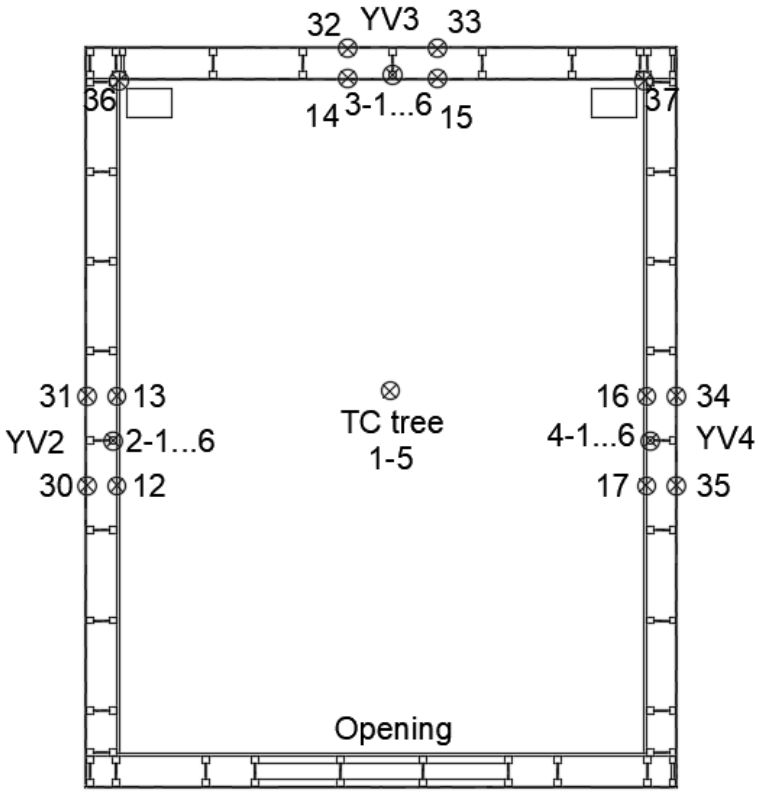

Figure 4.8 Thermocouple placement in the walls

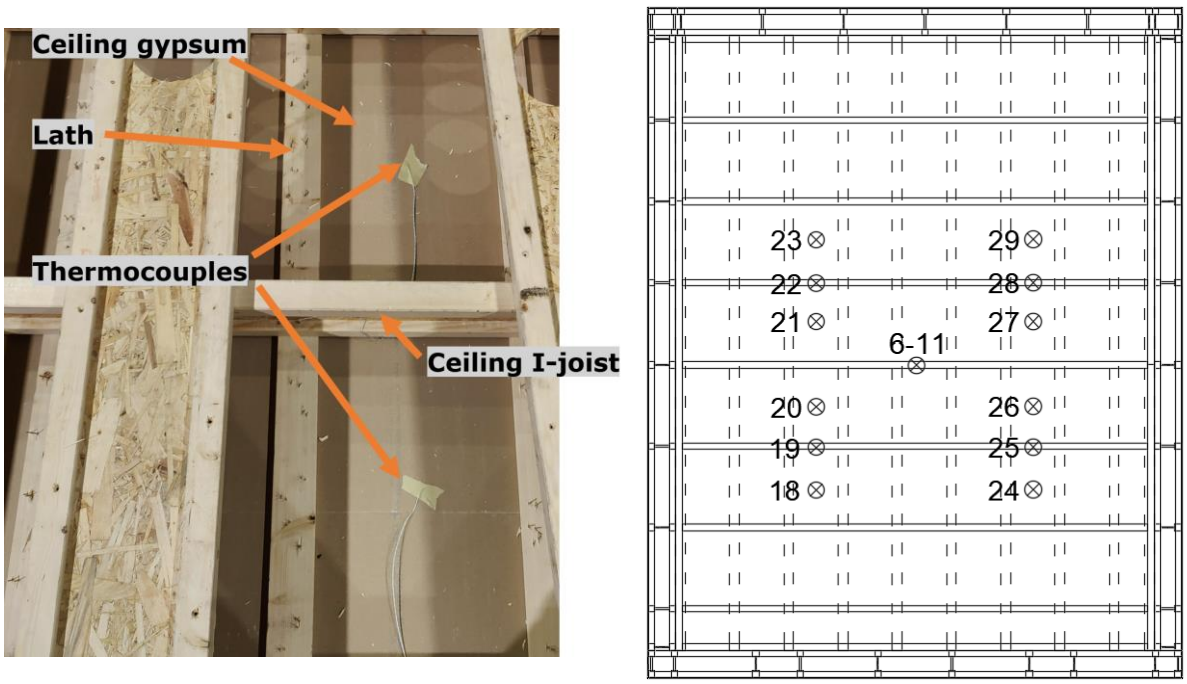

Figure 4.9 LEFT: Thermocouple placement on the ceiling (view from top); RIGHT: TC positions on the ceiling

A thermocouple tree, which had five different measurement points at different heights equidistant from each other was fastened with staples to the ceiling. The TC tree was in the middle of the room between the stacks of wooden pallets. The approximate location of the thermocouple tree in the plan can be seen in Figure 4.8. The lowest TC was number 1 and the highest was 5.

A heat flux sensor and a plate thermocouple with a TC behind it were placed approximately 2 meters high and 7 meters in front of the opening. This is to simulate a possible neighbouring building and to determine the amount of heat a compartment fire could cause. In this thesis the data from these instruments are not analysed.

4.3 Designed fire scenario

The fire load inside the compartment was designed to be 550 MJ/m^2. The initial calculation of the fire load was done by a RISE specialist. The wooden pallet heat of combustion was chosen approximately because the exact moisture of the pallets was not measured. The heat of combustion value for the pallet was chosen 16,7 MJ/kg. Wooden pallets were chosen for the fire load due to the ease of obtaining them. The wooden pallets were weighed, and the fire load could be calculated.

The GLT was not taken into account in the initial fire load calculation. If the GLT columns are considered in the fire load of the compartment the value of it would be approximately 750 MJ/m^2 based on the following calculation:

The heat of combustion for the GLT would be ΔH = 20,4 MJ/kg. The density is ρ = 420 kg/m^3. Volume of two GLT columns:

$V = 2 * 2{,}4 * 0{,}3 * 0{,}2 = 0{,}288\, m^3$

The weight of the GLT:

$m = 420 * 0{,}288 = 121\, kg$

The possible heat load from the GLT:

$Q_{fi.k} = 121 * 20{,}4 = 2468\, MJ$

The GLT heat load density:

$q_{f.k} = \frac{2468}{15{,}75} = 156{,}7 \frac{MJ}{m^2}$

The pallet heat of combustion value would be 17,9 MJ/kg based on the SFPE Handbook of Fire Protection Engineering [15]. According to the new heat of combustion value of the pallet and the added GLT heat load the total heat load density would be:

$$q_{f.d} = 156{,}7 + 594 = 751\ \frac{MJ}{m^2}$$

The opening factor of the compartment is calculated according to the equation (2.33). $O = \frac{A_v\sqrt{h_{eq}}}{A_t} = \frac{3{,}188\sqrt{2}}{70{,}364} = 0{,}064\ m^{0.5}$

The 24 wooden pallets were placed in the middle of the room. Four equal number of pallet stacks were laid out equidistant from the walls as seen in Figure 4.10.

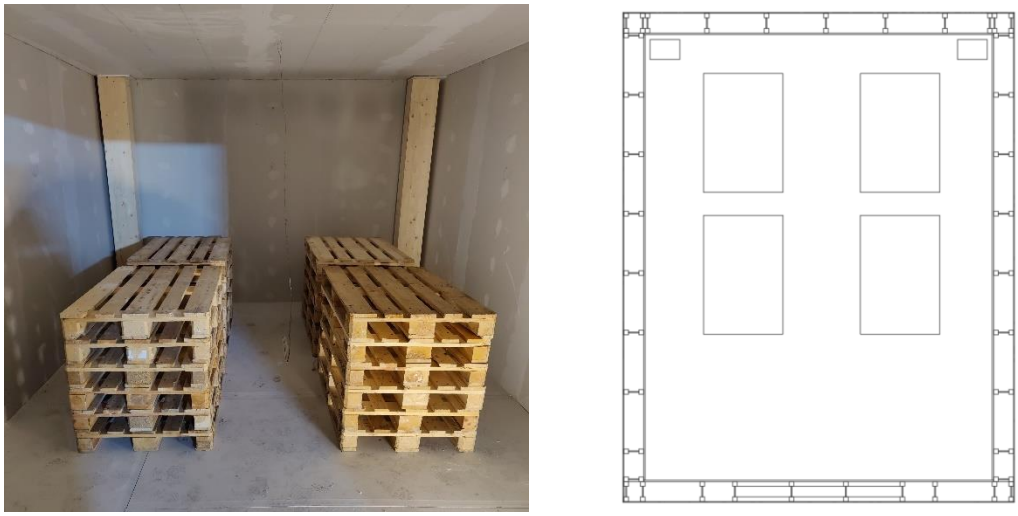

Figure 4.10 LEFT: Wooden pallets in the compartment; RIGHT: Approximate wooden pallet locations

A prediction of the compartment test is shown in Figure 4.11, which was made by Daniel Brandon from RISE. The graph shows two scenarios of the test with two different heat release rates (HRR). In ventilation-controlled fires, heat release rate depends on the air supply rate and the mass loss rate, in addition to other factors [15]. In the graph the flashover is predicted to take place at approximately 4 minutes. The fully developed fire lasts for about 15 minutes after which the decay phase begins. The graph does not account for the fire load of the GLT.

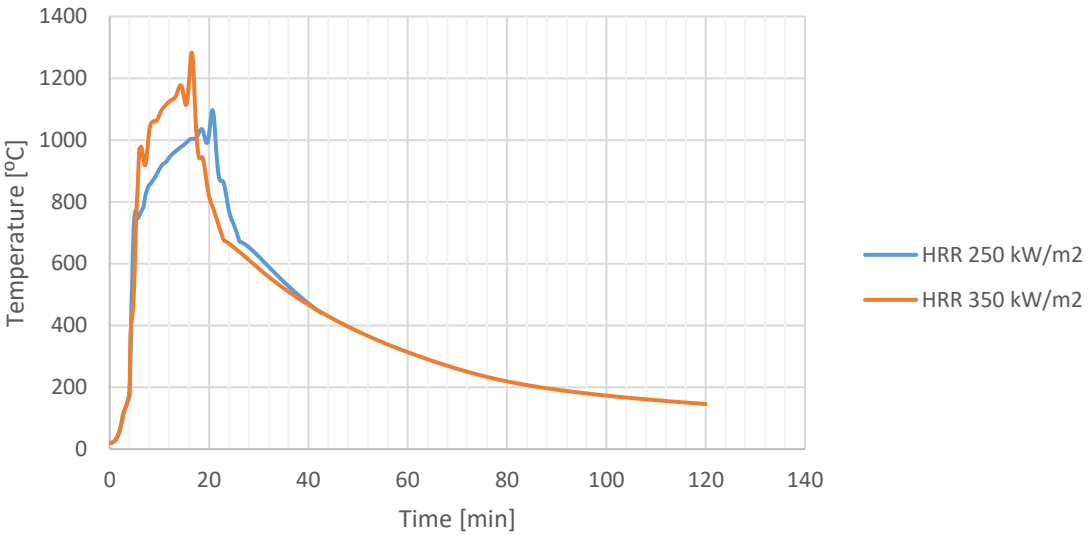

Figure 4.11 Heat release rate prediction by Daniel Brandon, RISE

5. RESULTS AND ANALYSIS

The test was led by RISE Fire research AS specialists. The test was carried out in a controlled and safe environment.

5.1 Timeline of the test

00:00 (mm:ss) Four wooden pallet towers are ignited. (Figure 5.1 left)
02:20 There are flames room high.
02:50 The flames are coming out of the opening
03:00 The flashover occurs.
07:00 Figure 5.1 right
09:00 The fire was most intense visually.
12:25 The maximum temperature 1292 °C is recorded by the thermocouple tree in the compartment. (Figure 5.2 left)
14:08 First pallet stack falls.
15:30 The fire is decaying visually – the flames are not as high and not as intense.
16:10 Flames can be seen in walls gypsum gap.
17:00 2 pallet stacks fall.
19:30 The flames are no longer coming out of the opening.
22:11 One of the ceilings GtF falls in one piece from the ceiling. (Figure 5.2 right)
28:50 Half panel of back wall gypsum falls leaving the back wall unprotected.
25:00 Figure 5.3 left
30:55 Multiple pieces of the ceiling gypsum fall from the ceiling leaving
37:30 Parts of the second layer ceiling gypsum fall leaving the ceiling unprotected from some points
40:30 More ceiling gypsum parts fall, ceiling laths and joists are on fire.
43:10 Figure 5.3 right
51:30 Extinguishing the compartment begins due to the possible danger of collapse.

Figure 5.1 LEFT: 00:15; RIGHT: 07:00

Figure 5.2 LEFT: 13:00; RIGHT: 22:11

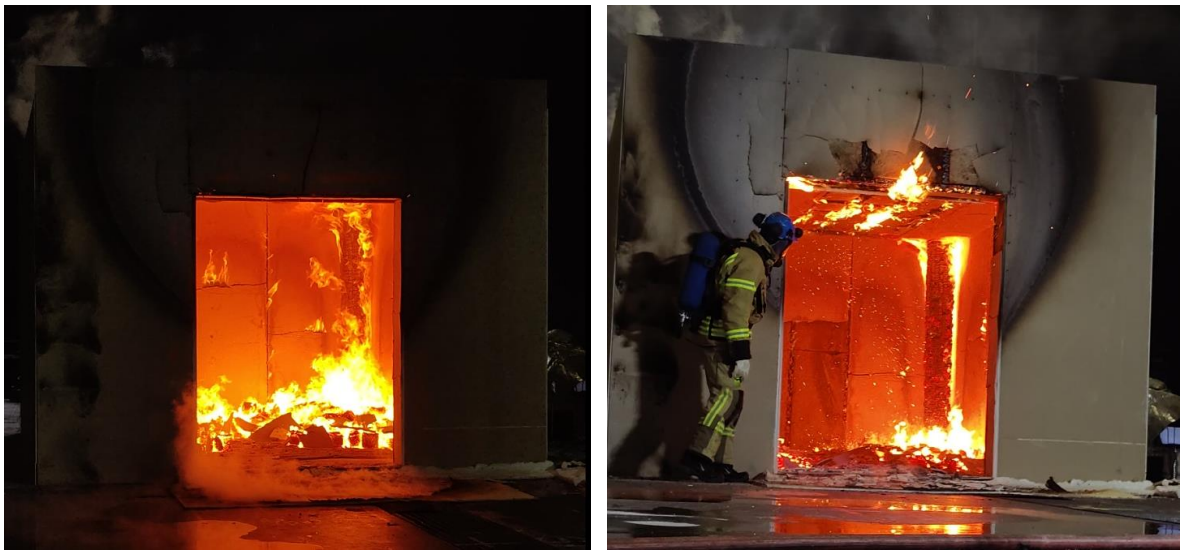

Figure 5.3 LEFT: 25:00; RIGHT: 43:10

5.2 Temperatures

The thermocouple tree data is depicted in the Figure 5.4. Based on the data the flashover begins at approximately 3 minutes, the decay starts at approximately 18 minutes. This corresponds to the observations of the compartment test. The thermocouple tree fell and some of the measurements were corrupted. Before the tree failing the graph show the stratification of the temperatures. The lowest TC 1 is about 200 °C lower than the highest TC. After the tree failure the thermocouples were laying in the remaining burning wooden pallets. The possible failing point of the tree can be seen in the graph at approximately 13 minutes. The peak temperature of the compartment was approximately 1290 °C.

After 29 minutes thermocouple 4 malfunctioned and showed only corrupted data which is omitted from this graph. The thermocouple 1 had a spike in temperatures compared to 2 and 3. The start of the spike in temperature is exactly at the time when the first GtF panel falls from the ceiling.

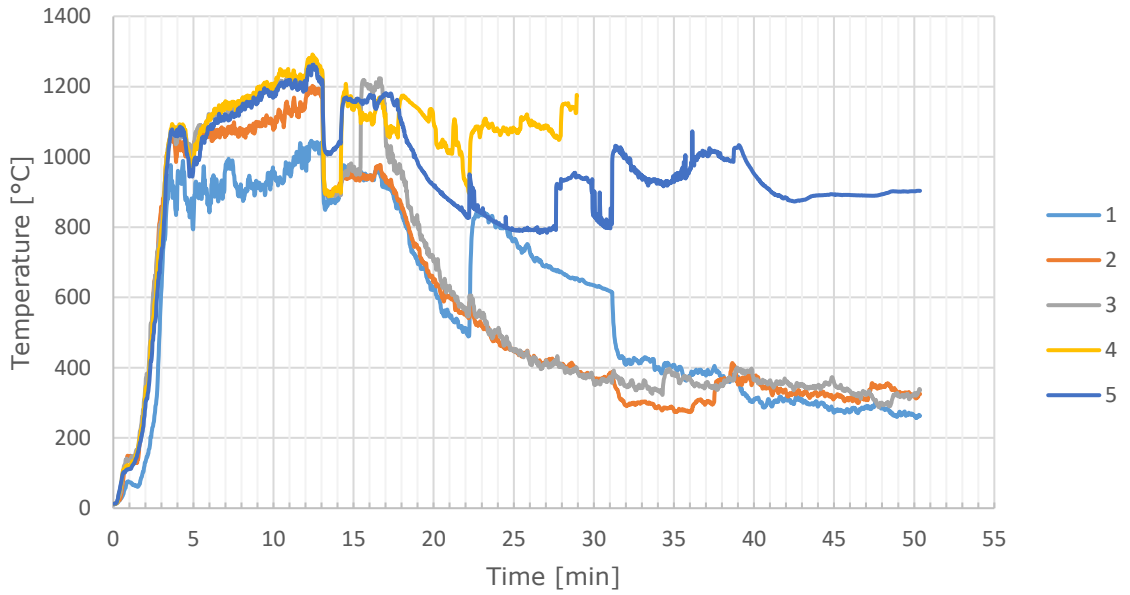

Figure 5.4 Thermocouple tree readings

After omitting the data from Figure 5.4 to give a more accurate depiction of the decaying phase and room temperatures without disturbances or hotspots and adding the ISO 834 temperature-time curve and the prediction done by Daniel Brandon in the same graph, similar temperatures and phases are shown in Figure 5.5.

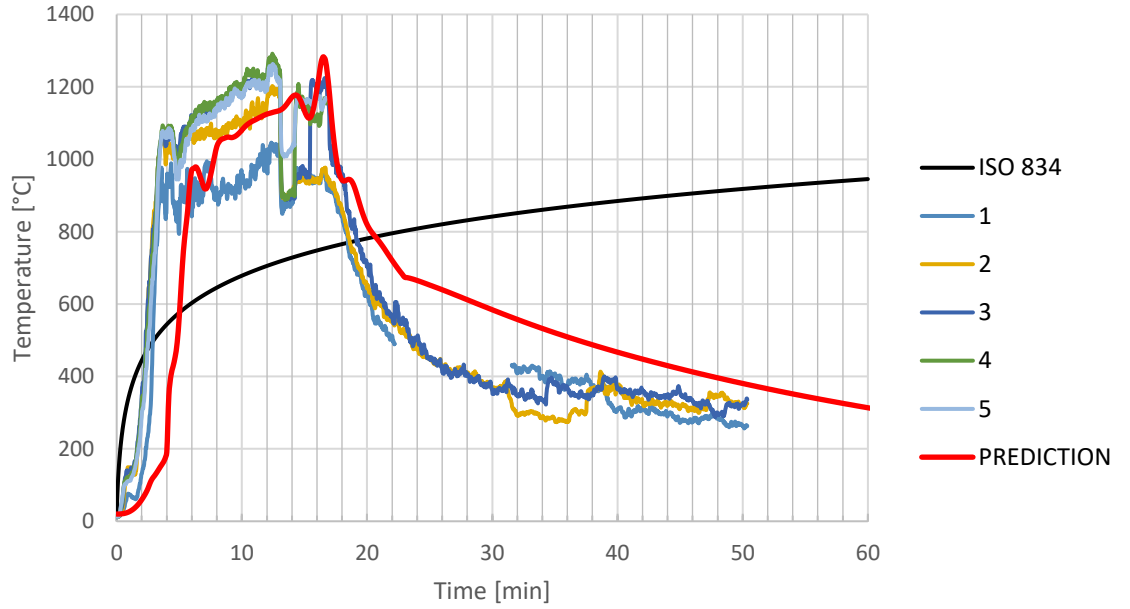

Figure 5.5 Thermocouple readings above the ceiling gypsum

The fully developed phase, maximum temperatures are quite similar. In the prediction the flashover starts approximately 2 minutes later. There is a distinctive spike right after the flashover in both the test and the prediction. The decaying phase start at about the same time in both of the situations but the decay is slower in the prediction.

A comparison between the measured temperatures, the prediction and the parametric temperature-time curve described in 2.2 are depicted in Figure 5.6. One of the lines includes the fire load of the GLT, the other one does not. The heating phase and the maximum temperatures are somewhat similar in all the curves except the one based on ISO 834. The difference between the parametric lines is the start of the decaying phase. In both figures the decay rate is the same. The decay rate in a parametric fire is corresponding to the fire growth – the faster the fire grows the faster it decays. When comparing the parametric temperature-time curve calculations the one which does not include the CLT fire load is closer to the real-life and the prediction scenarios, yet it is still far off from the other data due to the constant rate of decay.

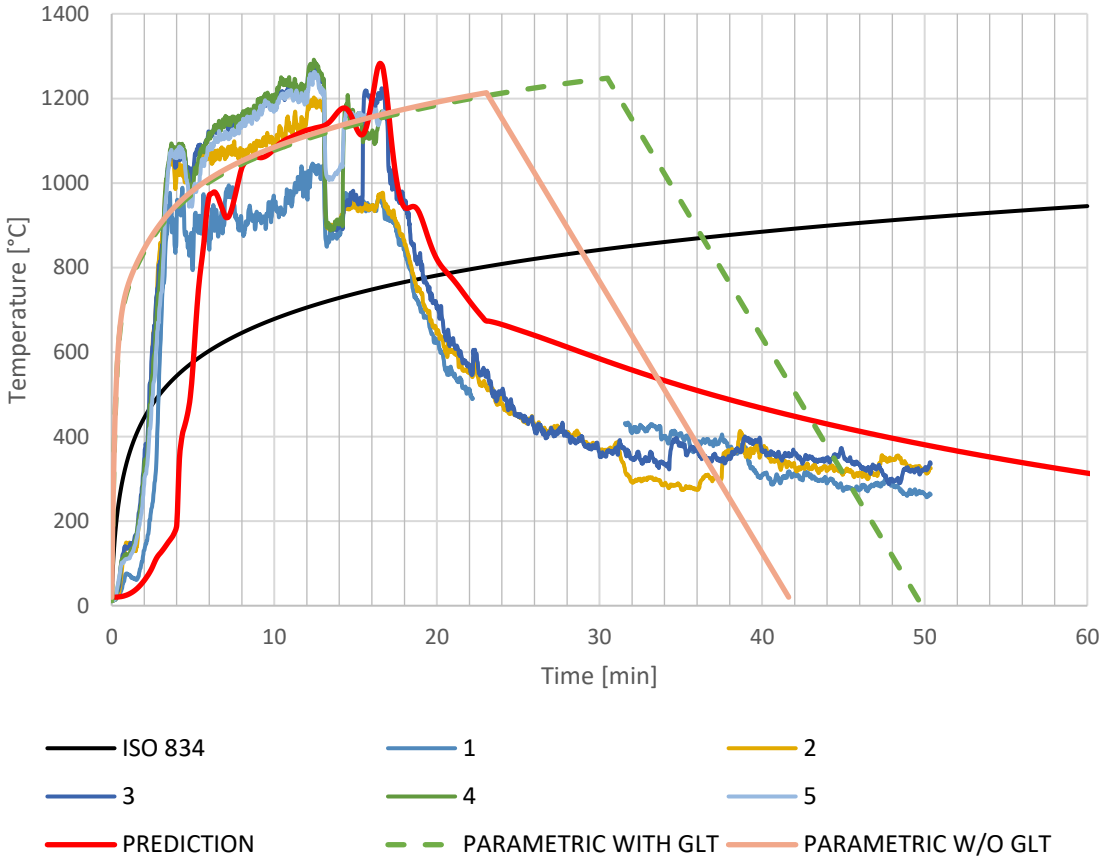

Figure 5.6 Parametric temperature curve with the GLT fire load

The prEN 1995-1-2:2025 gives a calculation model in which structural fire load from the timber can be determined from charring depth calculated based on the parametric temperature-time curve. The fire load density is calculated iteratively by repeatedly calculating the charring depth until the depth at the end of the fire does not increase more than 0,5 mm [1]. This calculation was completed, and the results showed that

the GLT would burn out completely and that the fire load would be equal to the situation described in Figure 5.6.

The temperature measurements on top of the gypsum boards on the ceiling are shown in Figure 5.7. Thermocouple number 28 did not record any data and is omitted from this graph. Thermocouple 19 possibly recorded corrupted data from approximately 23 minutes. When comparing thermocouple 27 and reviewing the video of the test it is not possible that the thermocouple is in the temperature range lower than 100 °C. The disturbances beginning from 35 minutes are caused by high temperatures over the thermocouple wires. Thermocouples which are placed on left side of the compartment (18-23) grow slowly in temperature and do not show any spikes in the graph. Thermocouples on the right side gain higher temperature much earlier and with faster rate. This is possible due to both layers of the ceiling gypsum failing from the right side. Possible charring behind the non-failed gypsum started at approximately 45 minutes.

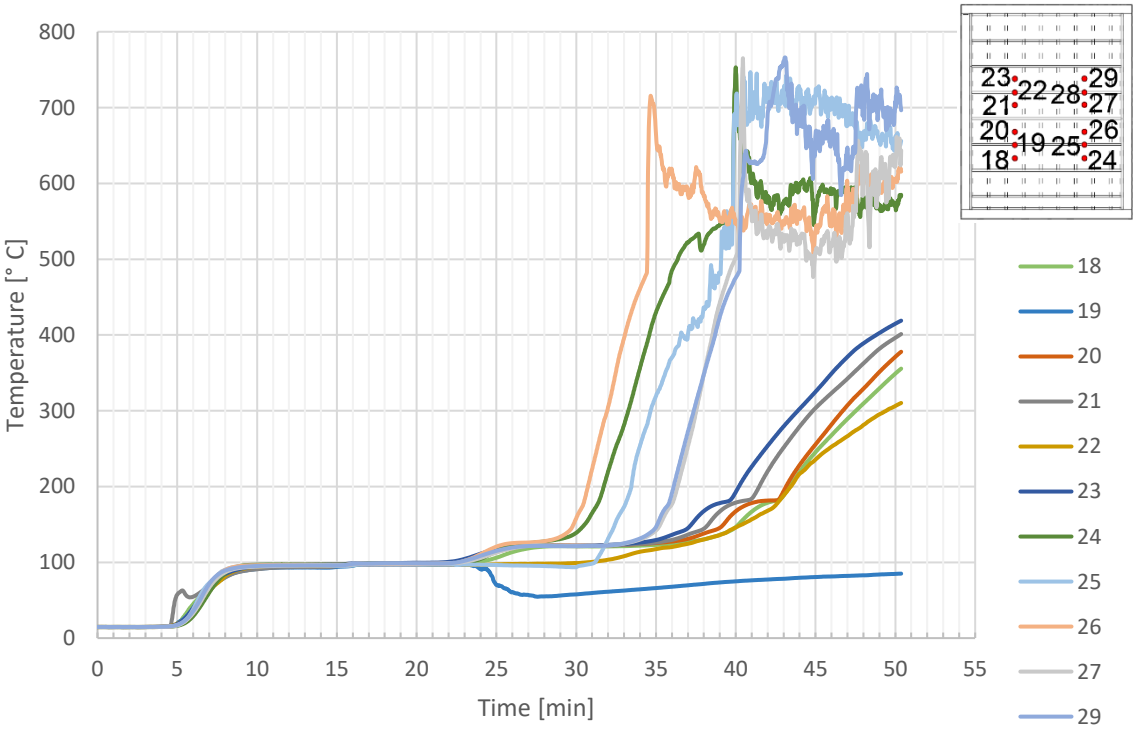

Figure 5.7 Thermocouple readings above the ceiling gypsum

The thermocouple readings behind the GLT are shown in Figure 5.8. The temperatures behind the GLT peaked at approximately 900 °C at about 40 minutes. After the peak both temperatures started to slowly decrease.

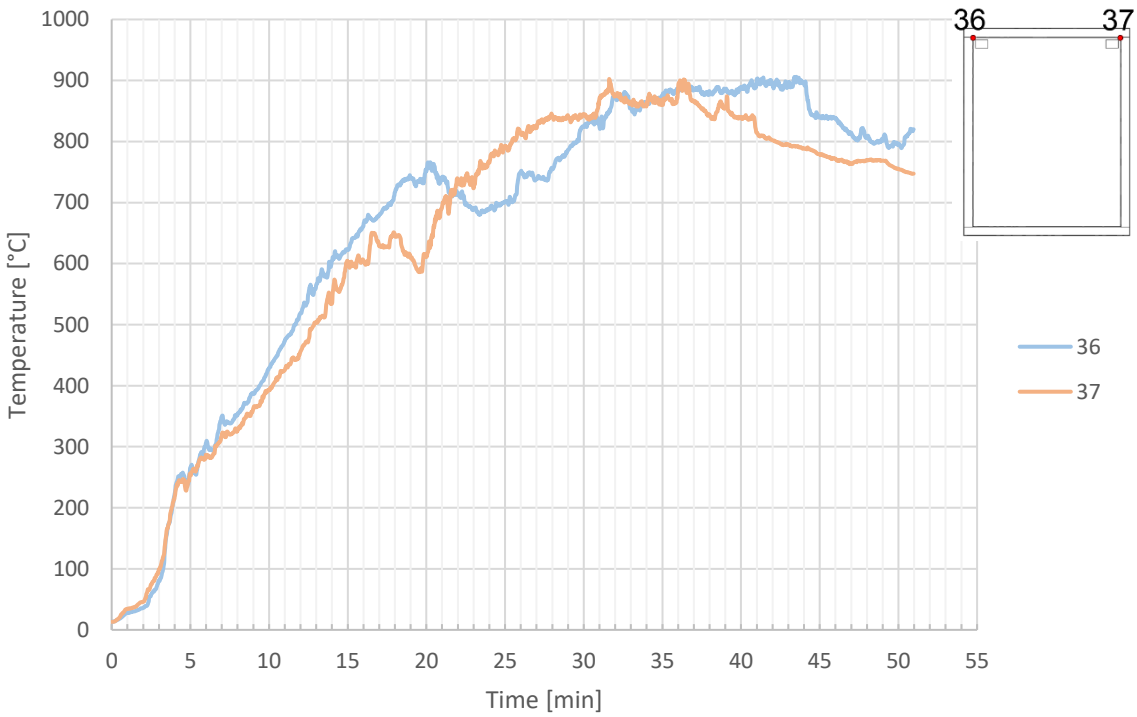

Figure 5.8 Temperatures behind the GLT in the innermost corners of the compartment

The thermocouple readings in the I-joists are shown in Figure 5.9, Figure 5.10 and Figure 5.11. The temperatures are very similar in growth and peak. At approximately 5 minutes after ignition the temperatures on the fire exposed side rise to 100 °C. At this stage the chemical reactions in the gypsum board start to develop and it protects the I-joist from the fire. The start time of charring on the fire exposed side is the time when thermocouple X-1 reaches 300 °C. When thermocouples X-5 or X-6 reach the same temperature is the start of lateral charring. Thermocouples X-2, X-3 and X-4 help calculate the charring rate on the fire exposed side which is calculated in chapter 5.5.2 I-joist charring depths.

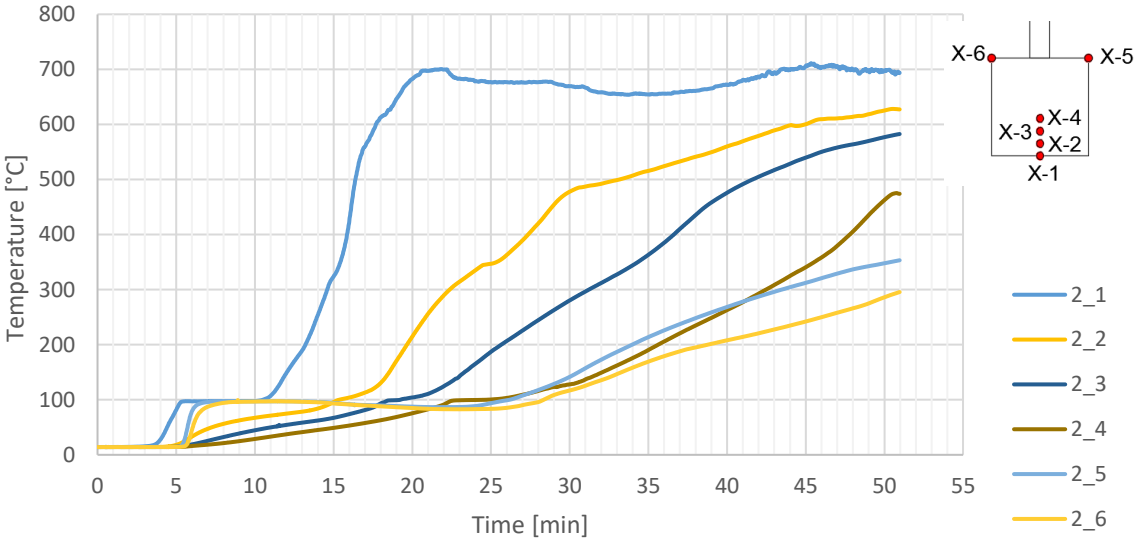

Figure 5.9 Thermocouple readings for I-joist in the wall YV2

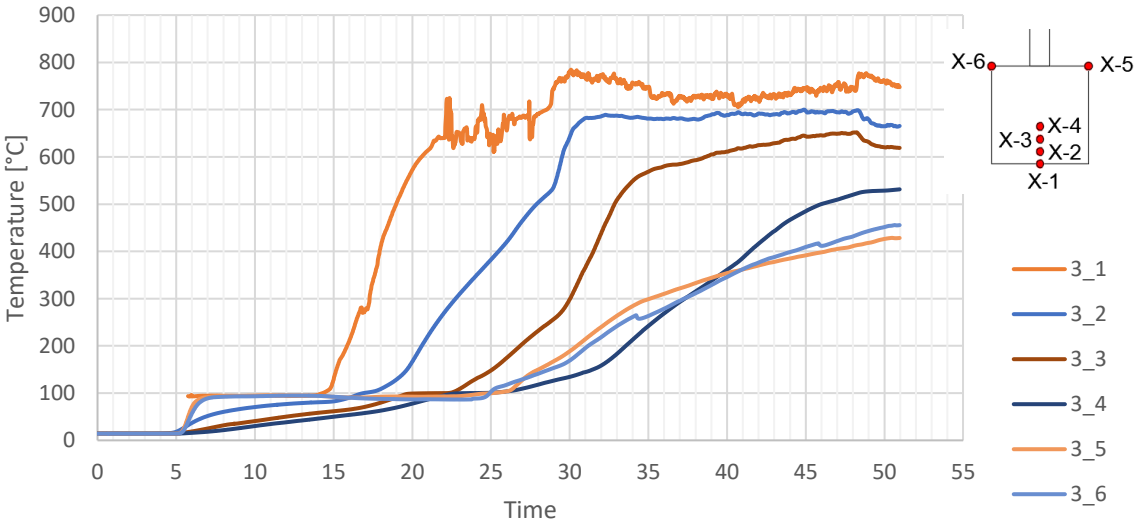

Figure 5.10 Thermocouple readings for I-joist in the wall YV3

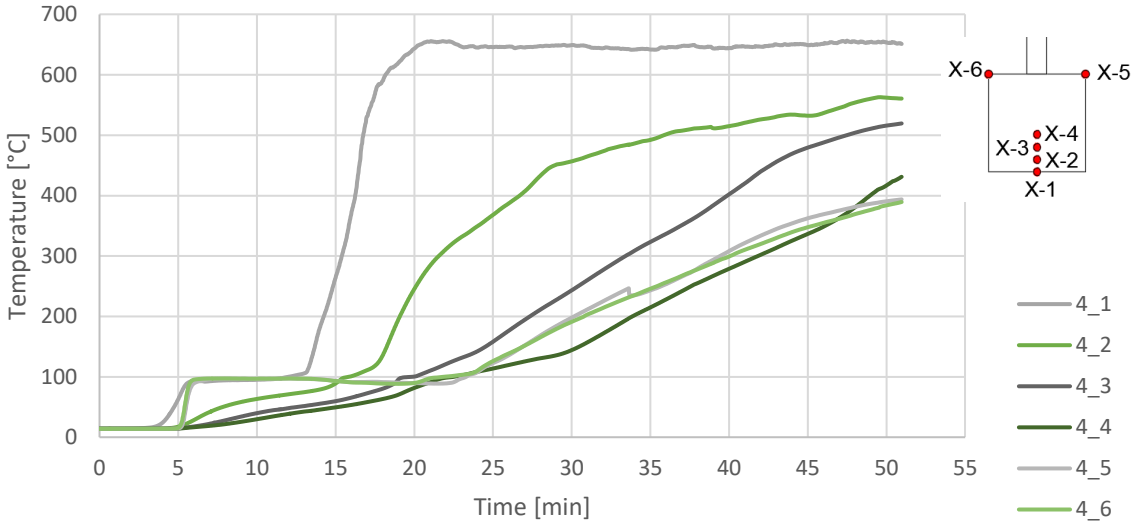

Figure 5.11 Thermocouple readings for I-joist in the wall YV4

The thermocouple readings for the I-joist in the ceiling are shown in Figure 5.12. The charring of the I-joist starts after approximately 34 minutes. At this time the big increase in temperature also shows the fall-off time of the gypsum beneath.

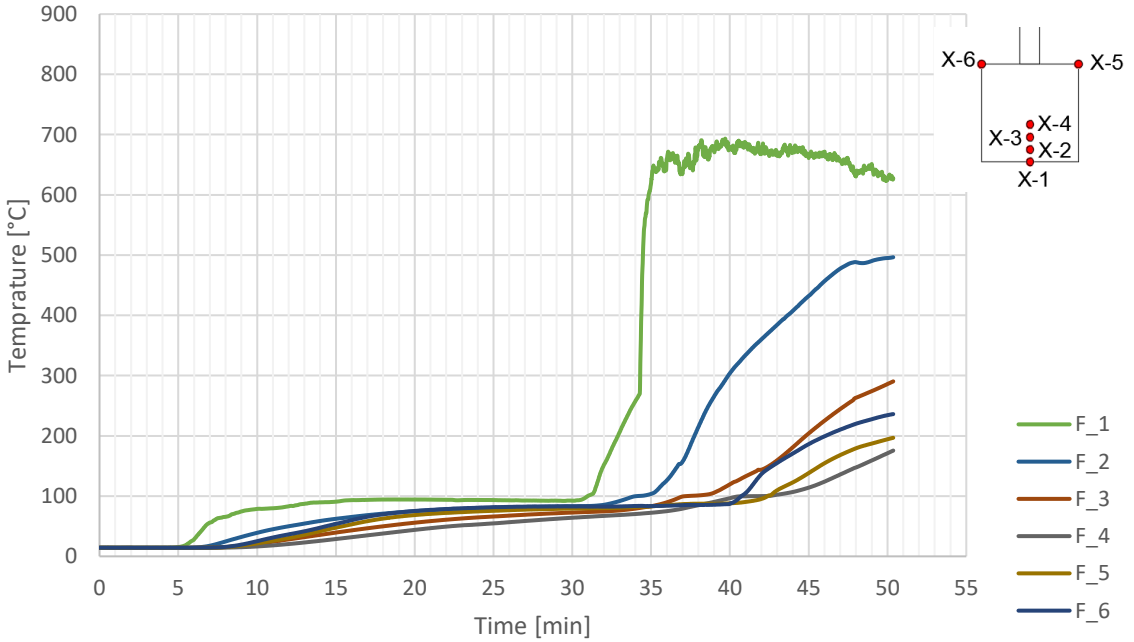

Figure 5.12 Thermocouple readings for I-joist in the ceiling

In Figure 5.13 the temperatures behind the gypsum board of the walls are shown. The temperatures are quite even and similar in values. From this figure it can be determined that the possible start time of charring behind the protective gypsum was approximately 15 minutes. The thermocouples 14 and 15 had a small spike in

temperatures at 29 minutes. At this time the gypsum board at those positions failed and fell on the ground in one piece.

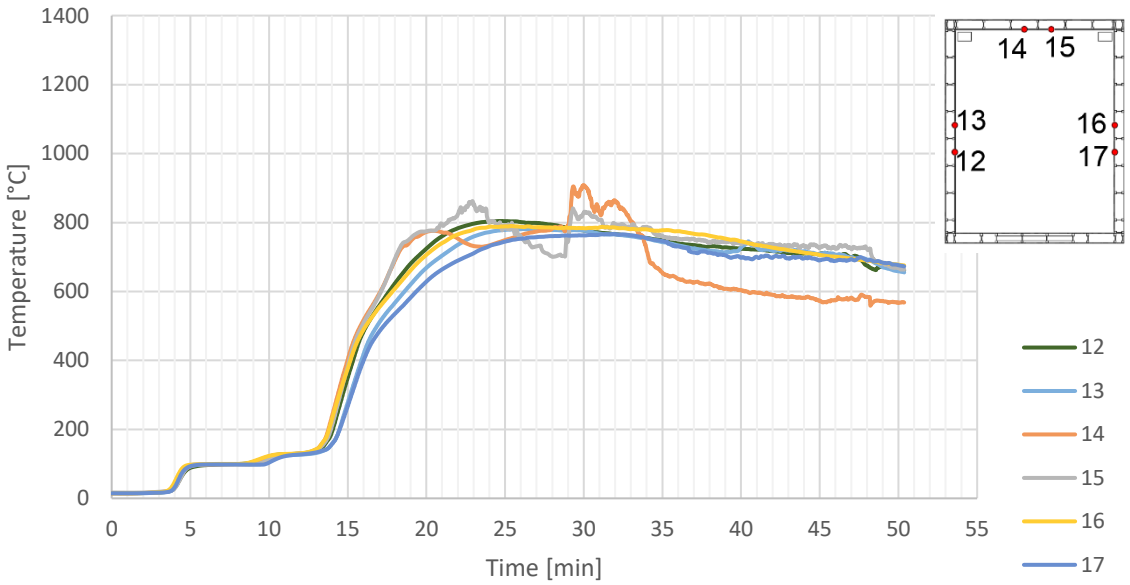

Figure 5.13 Thermocouple readings behind the wall gypsum next to measured I-joists

5.3 Residual cross-sections

The residual cross-sections were cut from four I-joists and both glulam columns. The cuts were made after the compartment was extinguished and cooled down completely. The wall I-joist cross-sections were cut close to the thermocouple positions. The slices were all approximately 3 cm thick. The residual cross-sections only describe the situation near the thermocouples as seen in Figure 4.8. The sections do not describe the charring of the whole compartment, for instance the right side of the compartment ceiling where the gypsum failed before the left. The wall I-joists which residual cross-sections were obtained placed behind the vertical joint of GtF.

The residual cross-sections were scrubbed with a steel wire brush to remove excess char. Both sides of the remaining wood cross-sections were traced on paper to get an accurate result. The traced lines were scanned with a ruler next to it to insure the right scale for exact area measurements. In Figure 5.14 the residual cross-sections of I-joists can be seen. The dotted line represents the initial cross-section.

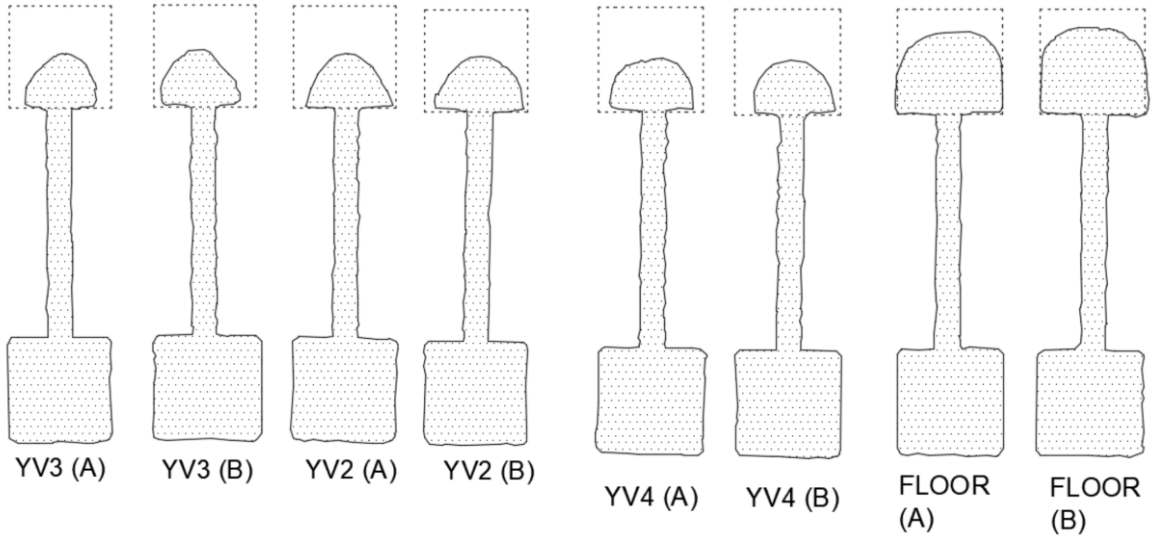

Figure 5.14 Residual cross-sections of I-joists

Figure 5.14 shows that the wall I-joists charring depths were quite similar. There was some lateral charring and approximately half of the flange height had charred. The floor I-joist didn't have any lateral charring and approximately a quarter of the height had charred. The exact residual flange heights and widths with charring depths can be found in Table 5.1. The flange width was measured from the widest points. The height of the flange was measured to the highest point of the residual cross-section.

Table 5.1 Residual flange dimensions

Position	Side	Height (mm)	Average height (mm)	Exposed side charring depth (mm)	Width (mm)	Average width (mm)	Lateral charring depth (mm)
YV2	A	25	25	22	40	40	3,5
	B	26			41		
YV3	A	25	25	22	33	34	6,5
	B	25			36		
YV4	A	23	23	24	37	36	5,5
	B	24			36		
FLOOR	A	37	37	10	47	47	0,0
	B	38			47		

The residual cross-sections of the GLT are visible in the Figure 5.15.

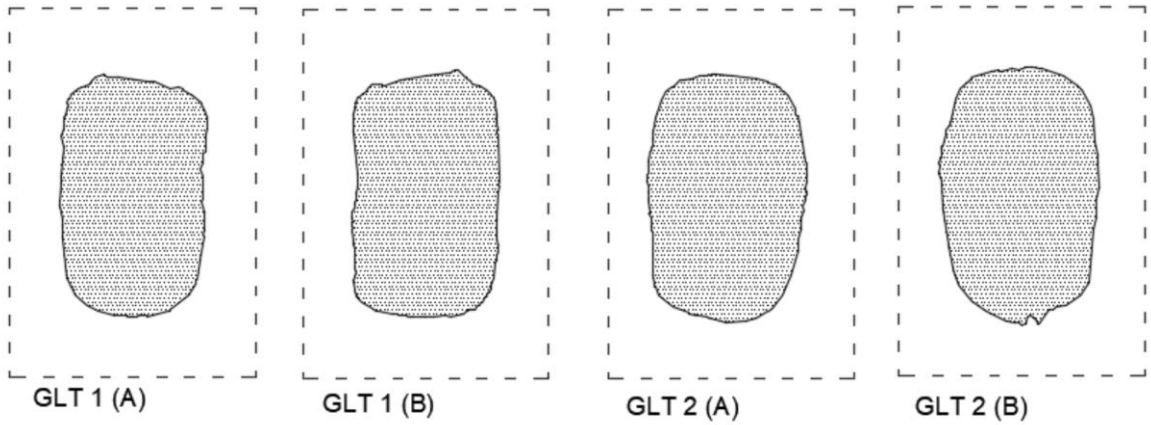

Figure 5.15 Residual cross-sections of the GLT

The dotted line represents the approximate area of the initial cross-section. The GLT may not have charred equally from every side due to temperature differences caused by the nearby wall. In the Figure 5.15, it can be seen that a big part of the cross-section area has charred. The residual dimensions of the GLT are provided in Table 5.2.

Table 5.2 Residual GLT dimensions and areas

Position	Side	Height (mm)	Average height (mm)	Width (mm)	Average width (mm)	Area (mm^2)	Average area (mm^2)
GLT1	A	197	198	115	115	21509	20975
	B	200		115		20441	
GLT2	A	200	204	130	129	22064	22217
	B	208		128		22369	

5.4 Comparison to standard fire

A comparison between the compartment test to prEN 1995-1-2:2025 is given in this chapter. The calculations are based on the standard times of charring provided by the standard and the charring and fall-off times which happened in the compartment fire test based on the TC and visual data.

5.5.1 GLT charring depths

Equations (2.1)-(2.3) were used to calculate the charring depth of the GLT. The time of charring is the duration of the test which is t = 50,4-2,5=47,9 min. The time from the ignition to the flashover is removed due to no charring occurring at that time.

$\beta_n = k_{gd} k_n \beta_0 = 1 * 1{,}08 * 0{,}65 = 0{,}702\ mm/min$

$d_{char,n} = \beta_n t = 0{,}702 * 47{,}9 = 33{,}6\ mm$

The residual height and width for the GLT:

$h = 300 - 2 * 33{,}6 = 232{,}7\ mm$

$b = 200 - 2 * 33{,}6 = 132{,}7{,}2\ mm$

The area of the residual GLT cross-section in a standard fire situation:

$A = 229{,}2 * 129{,}2 = 30897\ mm^2$

Table 5.3 The residual GLT cross-section area

Position	Residual height (mm)	Residual width (mm)	Residual area (mm^2)	Average charring rate (mm/min)
GLT1	198	115	20975	0,975
GLT2	204	129	22217	0,872
EC5	229	129	30897	0,702

As seen in Table 5.3 the residual area for the GLT cross-section in a standard fire exposure based on the prEN 1995-1-2:2025 is a lot bigger. This is due to the temperature in the compartment which was much higher compared to a standard temperature curve based on ISO 834. The GLT in the compartment test charred at a higher rate which is to be expected due to the nature of the fire.

5.5.2 I-joist charring depths

The I-joist charring depths were calculated according to equations provided in 2.1.2 Fire design of I-joists (equations (2.4) to (2.30)). The calculation of the web charring is not covered in this thesis because there were no I-joists which charred from the web.

The charring depth of wall I-joist flanges is calculated based on the standard fire exposure according to the charring and gypsum failure times provided by the prEN 1995-1-2:2025. Behind the 15 mm GtF the start time of charring is t_{ch} = 22 min. The according failure time is $t_{f,pr}$ = 44 min. The basic design charring rate for the I-joist flange is β_0 = 0,65 mm/min. [1]

To calculate the notional charring rates of the I-shaped timber member the start time of charring on the lateral side $t_{ch,2}$ is needed. Using the equations (2.20) to (2.30) the start time of charring on the lateral side $t_{ch,2}$ is calculated.

The basic protection time for the GtF (2.22):

$$t_{prot,0,i} = 30\left(\frac{h_i}{15}\right)^{1,2} = 30\left(\frac{15}{15}\right)^{1,2} = 30\ min$$

Position coefficient for the unexposed side of the GtF (2.26):

$$k_{pos,unexp,i} = 0{,}5 \cdot h_i^{0,15} = 0{,}5 \cdot 15^{0,15} = 0{,}751$$

The protection time of the GtF layer (2.21):

$$t_{prot,i} = \left(t_{prot,0,i} \cdot k_{pos,exp,i} \cdot k_{pos,unexp,i} + \Delta t_i\right) \cdot k_{j,i} = (30 \cdot 1 \cdot 0{,}751) \cdot 1 = 22{,}52\ min$$

The next layer of the assembly is the flange, mineral wool. The basic protection time for this layer (2.23):

$$t_{prot,0,i} = 0{,}3 \cdot h_i^{\left(0{,}75 \cdot log(\rho_i) - \frac{\rho_i}{400}\right)} = 0{,}3 \cdot 47^{\left(0{,}75 \cdot log(29) - \frac{29}{400}\right)} = 15{,}48\ min$$

The exposed side coefficient (2.25):

$$k_{pos,exp,i} = 0{,}5\sqrt{\frac{t_{prot,0,i}}{\sum t_{prot,i-1}}} = 0{,}5\sqrt{\frac{15{,}48}{22{,}5}} = 0{,}415$$

The unexposed side coefficient (2.27):

$$k_{pos,unexp,i} = 0{,}18 \cdot h_i^{(0{,}001\rho_i + 0{,}08)} = 0{,}18 \cdot 47^{(0{,}001 \cdot 29 + 0{,}08)} = 0{,}274$$

The protection factor for Phase 2 (2.15):

$$k_2 = 1 - \frac{h_p}{55} = 1 - \frac{15}{55} = 0{,}727$$

The maximum protection time of the layer (2.29):

$$t_{prot,max,i} = \frac{t_{prot,0,i}}{k_2} = \frac{15{,}48}{0{,}727} = 21{,}3 \leq \Delta t_{max,i}$$

The maximum correction time of the layer (2.30):

$$\Delta t_{max,i} = t_{prot,max,i} - t_{prot,0,i} \cdot k_{pos,exp,i} \cdot k_{pos,unexp,i} \cdot k_{j,i} = 21{,}3 - 15{,}48 \cdot 0{,}415 \cdot 0{,}274 \cdot 1 = 19{,}5\ min$$

The correction time of the layer (2.28):

$$\Delta t_i = \frac{\left(t_{f,pr} - \sum t_{prot,i-1}\right)\Delta t_{max,i}}{t_{prot,max,i}} = \frac{(44 - 22{,}5)19{,}5}{21{,}3} = 19{,}7\ min$$

The protection time of the layer (2.21):

$$t_{prot,i} = \left(t_{prot,0,i} \cdot k_{pos,exp,i} \cdot k_{pos,unexp,i} + \Delta t_i\right) \cdot k_{j,i} = (15{,}48 \cdot 0{,}415 \cdot 0{,}274 + 19{,}7) \cdot 1 = 21{,}47\ min$$

The start time of charring for the lateral side (2.20):

$$t_{ch,2} = \sum t_{prot,i-1} + t_{prot,i} = 22{,}52 + 21{,}47 = 44\ min$$

The calculation of the charring rate starts with determining the needed factor values as follows: the combined conversion and section factor for the fire exposed side (2.13):

$$k_{s,n,1} = 9{,}48 \cdot b_f^{-0{,}43} = 9{,}48 \cdot 47^{-0{,}43} = 1{,}811$$

The combined conversion and section factor fort the lateral side (2.14):

$$k_{s,n,2} = 2{,}25 \cdot h_f^{-0{,}13} = 2{,}25 \cdot 47^{-0{,}13} = 1{,}364$$

The post-protection factor for Phase 3 for the fire exposed side (2.16):

$$k_{3,1} = 6{,}5 - \frac{t_{f,pr}}{25} = 6{,}5 - \frac{44}{25} = 4{,}740$$

The post-protection factor for Phase 3 for the lateral side (2.17):

$$k_{3,2} = 0{,}01 + \frac{\max\left(t_{f,pr}; t_{ch,2}\right)}{338} = 0{,}01 - \frac{44}{338} = 0{,}140$$

The consolidation time (2.19):

$$t_a = 1{,}04 \cdot t_{f,pr} = 1{,}04 \cdot 44 = 45{,}76\ min$$

The factor for Phase 4 (2.18):

$$k_4 = 0{,}9 - \frac{t_a}{48} = 0{,}9 - \frac{45{,}76}{48} = 1{,}853$$

For each phase the notional charring rate can be calculated (based on formulae (2.8) to (2.12)).

$\beta_n = k_2 \cdot k_{s,n,1} \cdot \beta_0 = 0{,}727 \cdot 1{,}811 \cdot 0{,}65 = 0{,}856\ mm/min$ for the fire exposed side (P2)

$\beta_n = k_2 \cdot k_{s,n,2} \cdot \beta_0 = 0{,}727 \cdot 1{,}364 \cdot 0{,}65 = 0{,}645\ mm/min$ for the lateral side (P2)

$\beta_n = k_{3,1} \cdot k_{s,n,1} \cdot \beta_0 = 4{,}740 \cdot 1{,}364 \cdot 0{,}65 = 5{,}578\ mm/min$ for the fire exposed side (P3)

$\beta_n = k_{3,2} \cdot k_{s,n,2} \cdot \beta_0 = 0{,}140 \cdot 1{,}364 \cdot 0{,}65 = 0{,}165\ mm/min$ for the lateral side (P3)

$\beta_n = k_4 \cdot k_{s,n,1} \cdot \beta_0 = 1{,}853 \cdot 1{,}811 \cdot 0{,}65 = 2{,}181\ mm/min$ for the fire exposed side (P4)

The notional charring depths is calculated according to formulae (2.6) and (2.7). According to the design model in Figure 2.1 the calculation is as follows:

$d_{char,n,1} = \sum_{Phases}(\beta_n \cdot t) = \big(0{,}856 \cdot (44 - 22)\big) + \big(5{,}578 \cdot (45{,}8 - 44)\big) + \big(2{,}181(50{,}4 - 45{,}8)\big) = 38{,}8\ mm$

$d_{char,n,2} = \sum_{Phases}(\beta_n \cdot t) = \big(0{,}165 \cdot (50{,}4 - 44)\big) = 1{,}06\ mm$

Since the charring on the fire exposed side of the flange started before the table value of the EC5, calculation results with the compartment test data are given in Table 5.4. The differences are between the start time of charring and for the back wall also the gypsum fall off. The row "EC5 wall" is based on the tabular values of the prEN 1995-1-2:2025 and was described above in detail.

Table 5.4 The characteristic times and charring depths of the flanges from the calculations

	t_{ch}	$t_{f,pr}$	$t_{ch,2}$	$d_{char,n}$	$d_{char,n,2}$
EC5 wall	22	44	44	38,8	1,07
EC5 YV2	14,6	44	43,8	45,1	1,18
EC5 YV3	17,3	28,5	29,8	53,9	13,31
EC5 YV4	15,4	44	43,8	44,4	1,18

Based on the calculations the I-joist flange in the wall YV3 chars completely and no residual flange is left. This however does not happen in the test.

The calculations show less charring on the lateral side (excluding YV3). This is due to the gypsum not failing in the test. The residual sections were cut from the I-joists which were behind the vertical joint of the gypsum it cannot be compared to the calculation directly. The gap could have a small influence the protection capabilities of the protective system even though there is no void behind it. It is evident from the calculations from the wall YV3 that the earlier the gypsum fails the more lateral charring occurs. It should be noted that the $d_{char,n}$ value of YV3 shows the theoretical depth of the charring – the flange in the calculation chars completely.

The various charring depths for the lateral side of the flange are shown in Figure 5.16. The calculations are depicted with a solid line on the graph, the test with a dotted line. It can be seen that after the failure of the protection system the charring rate increases drastically. The calculation depth which reached about 45 mm for YV2 and YV4 are based on the temperature-time curve of the standard fire.

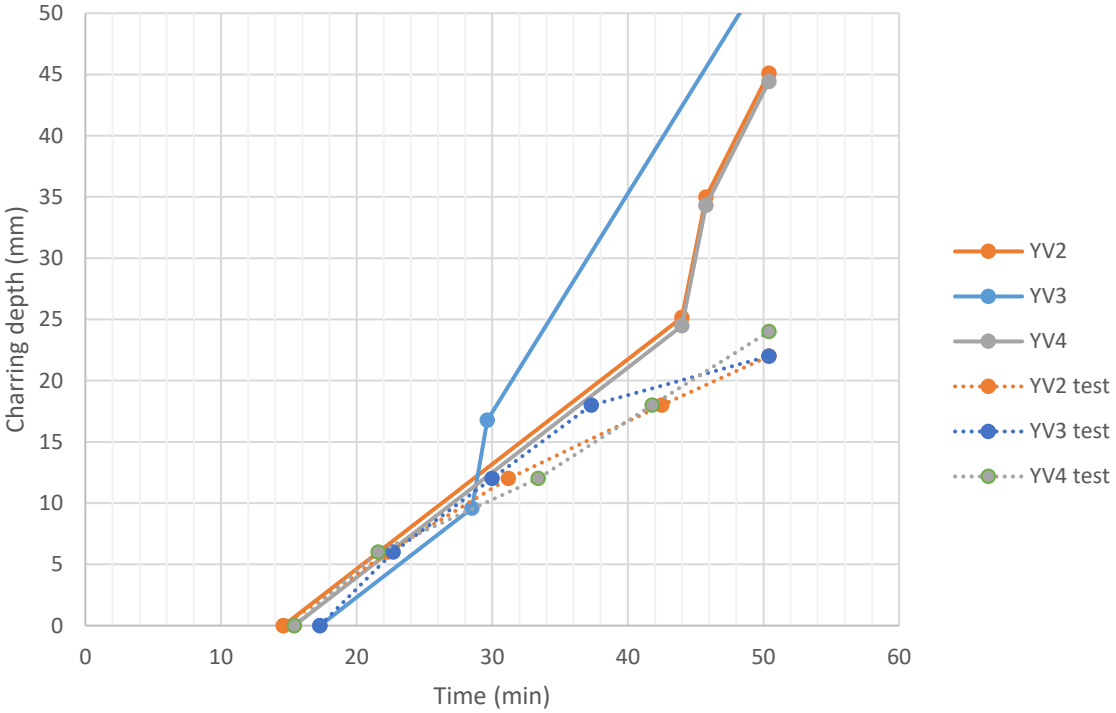

Figure 5.16 Charring depths based on the ECT5 calculations and the test

When the calculations are compared to the natural fire of the compartment, it is evident that the calculations are on the safe side (more charring occurs). For YV3 the protection failure is apparent in the charring rates. In the calculation model the big increase in depth is right after the gypsum failure. In the test there is a small increase in the charring depth compared to the other walls.

The floor charring calculation results are provided in Table 5.5. The start time of charring is determined by the I-joist thermocouple. To get comparable results to the test, the failure time of the fire protection system is the same as in the test.

Table 5.5 The characteristic times and charring depths of the flanges from the calculations

	t_{ch}	$t_{f,pr}$	$t_{ch,2}$	$d_{char,n}$	$d_{char,n,2}$
EC5 floor	45	56	56,8	3,2	0
EC5 test floor	34,3	34,3	35,72	36,8	2
Test	34,3	34,3	50,4+	10,0	0

The I-joist charred 10 mm from the lateral side in the test which shows that the calculation model is again on the safe side quite significantly. The reality of the situation is that the exact location of the cut residual cross-section is unknown. Due to the half of the ceiling gypsum failure the cross-section could have been cut behind the gypsum (which is highly unlikely, due to the charring rate), right next or behind the failed gypsum. Based on the calculations with the EC5 draft, if the gypsum does not fail but the charring starts at 34,3 minutes then the charring values would be: $d_{char,n}$ = 6 mm with no lateral charring. When comparing the tabular charring start time of the I-joist to the compartment test it can be seen that the charring starts at the right time. According to Figure 5.7 the charring start time behind the non-failed gypsum is approximately 45 minutes or even later.

In the ceiling, a GtF board failed before the failure time described in prEN 1995-1-2:2025 which ultimately led to the GtA board failing earlier than it should when compared to standard fire. There can be multiple reasons for this. Firstly, the gypsum boards could have had mechanical damage which could not be seen by eye. This could have led to the early failure for certain boards. Secondly, the staples with which the gypsum boards were fastened were not fastened properly. This was due to human error – some of the staples didn't hit the laths in the right place. After reviewing pictures of the construction, it is evident that on one of the laths some of the staples were not fastened in the correct position as seen in Figure 5.17. This mistake is visible almost in full length of the lath.

Figure 5.17 Staples missing the lath

5.5 Comparison to compartment tests

The compartment was built to be comparable to previous tests. The floor area is the same as in Hakkarainen, McGregor, Li et al. and Hevia tests. The opening factor of the built compartment is 0,064 $m^{1/2}$ which is bigger than the compared to the other tests due to the size of the opening. This means that the performed test was more ventilation controlled and less fuel controlled compared to other tests. Due to this fact the fire was more volatile.

The flashover in the performed test happed in 3 minutes. None of the compared tests had a flashover so fast, the fastest time to flashover was 4 minutes in Hevia tests. The peak temperature of the compartment was 1290 °C which is also slightly higher than the tests in the overview. The rapidly developed fire could be explained due to the type of ignition used. In the performed compartment there were special ignition cubes and all of the pallets were ignited at the same time. The ignition cubes and the big opening could have had an effect on the time when the flashover happened.

The start of decay time is most similar to tests conducted by Hevia. The performed test had a decay start approximately 18 minutes compared to the tests by Hevia which had a start time of 20 minutes. The gypsum fall off when compared to light steel compartments test performed are not as severe. Falling of the gypsum for light

steel frame assemblies could cause failure of the construction and exterior board failure [6]. In the performed test some of the gypsum on the walls failed, but mostly it stayed in place. There was no open fire seen on the exterior side of the compartment. This means the joints of the compartment did not fail.

The charring of the I-joists is comparable to the light timber frame test conducted by Li et al. The average charring rate behind the walls YV2 and YV4 where the gypsum did not fail was 0,70 mm/min. The wall YV3 had a charring rate of 0,92 mm/min. These numbers are calculated from the thermocouple readings in the depths of 6, 12 and 18 mm. Compared to the tests conducted by other researchers the average charring rate of 0,70 mm/min is on par with other test which had protected surfaces.

Previous research has seen multiple flashovers due to the gypsum failing, especially in the CLT tests where ventilation was sufficient [6]. The encapsulated timber usually does not contribute to the compartment fire or the contribution is insignificant. This leads to an increased heat release rate. The contribution of exposed timber can lead to a delayed decay of fire. In the performed test the GLT columns in both back corners had an impact on the decay of fire which was seen on the data measured behind the GLT. More in depth analysis should be carried out on this subject.

The performed compartment test with I-joist was one of a kind and the author of this thesis did not find data on possible similar tests.

The problems encountered in this test was that the TC tree failed. This was possibly due to the fire load falling on the wiring. Previous tests have encountered tree failure due to the gypsum falling. This makes the thermocouple locations of the tree uncertain.

SUMMARY

The aim of this thesis was to analyse a compartment fire test with I-joists. The analysis is based on the data collected from the test conducted in Norway on 25th of March 2022. The author assisted in the building of this compartment and helped installing the instruments for data recording.

The performed test was successful yet did not provide the full information which was hoped in the first place. Due to the early failure of the ceiling gypsum the I-joists in the ceiling were on fire. Therefore, the team decided after 50 minutes from ignition that due to the need of residual cross sections the fire would be extinguished.

The analysis of the test involved making calculations based on the draft prEN 1995-1-2:2025 to give feed back to the authors of the I-joist calculation model. The calculations showed that when under similar time conditions the model provides a large margin of safety in the event of standard fire compared to a natural fire. The average charring rate behind the gypsum protection system of the flange on the fire exposed side was 0,70 mm/min. The charring behind the protection system for the wall started earlier compared to the charring start time provided in the standard. The I-joists in the ceiling did not char on the lateral side. Behind the intact gypsum the charring started at the time provided in the prEN1995-1-2:2025.

Different temperature-time curves were compared in this thesis. The standard ISO 834, the prediction from a simulation of the fire test and the parametric temperature-time curve in the EN 1991-1-2 were compared. The simulation was very similar to the real fire even though it did not consider the GLT columns in the compartment. The parametric curve had similar flashover speed and peak temperature.

An overview and analysis of similar compartment fire tests was provided. The test results were similar to comparable fire tests. The flashover happened earlier and the peak temperatures were slightly higher in the performed test.

To the knowledge of the author previous compartment fire tests with I-joists has not been carried out. More research on the charring and the structural strength in fire of I-joists in timber frame assemblies should be carried out to refine the fire design model for I-joists.

KOKKUVÕTE

Käesoleva magistritöö eesmärgiks oli uurida I-taladega teostatud ruumtulekahjukatse tulemusi. Läbiviidud analüüs põhineb 25. märtsil 2022 sooritatud katse andmetel. Antud töö autor osales katsekeha ehitusel ja abistas mõõteseadeliste paigaldamisel.

Läbiviidud katse oli edukas, kuid ei andnud täielikku informatsiooni, mida loodeti enne katset omandada. Kuna üks lae kipsplaat kukkus alla arvatust varem ja avas laetalad tulele, siis katse läbiviijate seas võeti vastu otsus kustutada tulekahju peale viiekümnendat minutit. Katse lõpetamise eesmärk oli vältida ruumi kokkuvarisemist ning et oleks võimalik lõigata jääkristlõikeid kandekonstruktsioonist.

Töö käigus võrreldi I-talade standardtulekahjujärgseid arvutusi standardi prEN 1995-1-2:2025 kavandi põhjal loomuliku tulekahju katsel saadud tulemustega. Standardtulekahju järgsed arvutuslikud söestumissügavused olid tunduvalt suuremad võrreldes katsega. Kaitsekihi taga oli keskmine söestumiskiirus seina I-tala vööl 0,70 mm/min. Seina I-tala söestumine kipsplaadi taga algas läbiviidud katses varem võrreldes standardist tuleneva ajaga. Ruumi laes olevad I-talad ei söestunud vöö külgedelt. Söestumine mitte alla kukkunud lae kipsi taga algas vastavalt standardis väljatoodud ajale.

Antud töös võrreldi erinevaid temperatuuri-aja sõltuvusi. Võrdluseid tehti ISO 834 standardi kohase standardtulekahju kõvera, ruumtulekahju simulatsioonil põhineva ennustuse ja EN 1991-1-2 poolt esitatud parameetrilise temperatuuri-aja graafiku vahel. Katse ennustuses esitatud ruumi õhutemperatuurid olid väga sarnased läbiviidud katses olnud temperatuuridele, kuigi ennustuses ei arvestatud ruumis olevate liimpuitpostide panust. Parameetrilise temperatuuri-aja graafikul olid läbi viidud katsega võrreldes tule temperatuur ja lahvatusperiood sarnased.

Töö ühe osana tehti ülevaade ja võrdlus varasemalt teostatud sarnaste ruumtulekahju katseandmetest. Läbiviidud katse tulemused olid sarnased varasematele teostatud puitkonstruktsioonidega ruumtulekahjukatsetele. Tule lahvatus toimus võrreldes teiste katsetega varem ning kõrgeim õhutemperatuur ruumis oli suurem.

Autorile teadaolevalt ei ole varasemalt samasuguseid ruumtulekahjukatseid I-taladega sooritatud. Edasine uurimistöö on vajalik I-taladest ehitatud kandekonstruktsioonide kohta erinevates tule olukordades, et täpsustada olemasolevaid arvutusmudeleid.

LIST OF REFERENCES

[1] prEN 1995-1-2:2025, "Eurocode 5: Design of timber structures, Part 1-2: Structural fire design", CEN TC250 SC5 WG4, Aug. 2022.

[2] K. N. Mäger, 'Preliminary design model for wooden I- joists in fire', p. 14, 2019.

[3] K. N. Mäger and A. Just, 'Improved fire design model for walls and floors with I-joists', Aug. 2022.

[4] ISO 834-1:1999, 'Fire-resistance tests - Elements of building construction - Part 1: General requirements', International Organization of Standardization.

[5] EN-1991-1-2:2004, 'Eurocode 1: Actions on structures, Part 1-2: General actions, Actions on structures exposed to fire'. European Committee for Standardization.

[6] D. Brandon and B. Östman, 'Fire Safety Challenges of Tall Wood Buildings – Phase 2: Task 1 - Literature Review', p. 46., Sept. 2016.

[7] T. Hakkarainen, 'Post-flashover fire in light and heavy timber construction compartments', *J. Fire Sci.*, vol. 20, pp. 133–175, Mar. 2002.

[8] EN 520:2004+A1:2009, 'Gypsum plasterboards - Definitions, requirements and test methods.', European Committee for Standardization.

[9] T. Lennon, D. Hopkin, J. El-Rimawi, and V. Silberschmidt, 'Large scale natural fire tests on protected engineered timber floor systems', *Fire Saf. J.*, vol. 45, no. 3, pp. 168–182, Apr. 2010, doi: 10.1016/j.firesaf.2010.02.006.

[10] A. R. M. Hevia and B. Eng, 'Fire resistance of partially protected cross-laminated timber rooms', p. 199.

[11] C. McGregor, 'Contribution of cross laminated timber panels to room fires', Master of Applied Science, Carleton University, Ottawa, Ontario, 2013. doi: 10.22215/etd/2013-06885.

[12] X. Li, X. Zhang, G. Hadjisophocleous, and C. McGregor, 'Experimental Study of Combustible and Non-combustible Construction in a Natural Fire', *Fire Technol.*, vol. 51, no. 6, pp. 1447–1474, Nov. 2015, doi: 10.1007/s10694-014-0407-4.

[13] 'ETA 12/0018', RISE Research Institutes of Sweden AB, Aug. 2018.

[14] IEC 584-1:1995, 'Thermocouples', International Electrotechnical Commission.

[15] National Fire Protection Association and Society of Fire Protection Engineers, Eds., *SFPE handbook of fire protection engineering*, 3rd ed. Quincy, Mass. : Bethesda, Md: National Fire Protection Association ; Society of Fire Protection Engineers, 2002.